

GYR
BLITZ



**26th Annual AHS Student Design Competition
Undergraduate Category**



Acknowledgments

We would like to recognize and thank the following individuals for their assistance in the completion of this design project:

Dr. Mark Costello
Dr. Daniel Schrage
Dr. Lakshmi Sankar
Dr. Kyle Collins
Mr. Marc Dalziel
Mr. James Tolbert IV

2009 Georgia Tech Undergraduate Blue Design Team



Collin Brown (BS Student, Georgia Tech)



Eric Singh (BS Student, Georgia Tech)



Fady Gaied (BS Student, Georgia Tech)



Priyam Gore (BS Student, Georgia Tech)




Thomas Keister (BS Student, Georgia Tech)



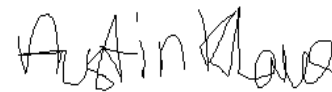
Robert Price (BS Student, Georgia Tech)



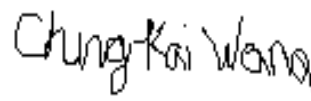
Robert Ruch (BS Student, Georgia Tech)



Tyler Trawick (BS Student, Georgia Tech)



Chung-Kai Wang (BS Student, Georgia Tech)



Austin Klaus (BS Student, Georgia Tech)

For participating in the 2009 AHS design competition, undergraduate students received academic credit for AE4359: Rotorcraft Design.

Executive Summary

The 2009 American Helicopter Society student design competition calls for a unique rotorcraft design which utilizes a highly innovative, non-conventional rotor/drive system. The main objective of these innovations is to endow the final design with improved performance in terms of speed, range, payload, endurance and noise signature. The Georgia Tech Undergraduate Rotorcraft Blue Design Team has responded with the development of the Gyroblitz.

The competition requires the selection of a benchmark helicopter to provide a comparative view and the Gyroblitz is a derivative of the Bell 412 EP rotorcraft. The Gyroblitz is a design built with the principal to innovate for the sake of performance, a clear distinction from innovation for the sake of innovation. At the same payload as the Bell 412, the Gyroblitz has a 17% increase in maximum speed, a 27% increase in cruise speed, a 16% increase in range, 7% increase in endurance speed, and as good of a noise signature as the Bell 412.

In hover the Gyroblitz is designed to use a powered main rotor and tail propeller. In forward flight the main rotor transitions to an auto-rotative state. In this state the aircraft is designed to utilize a variable-direction propeller providing forward thrust. The internal structure of the tail has been modified to utilize a carbon fiber shaft to reduce weight. A slip clutch system has been added to the drive train to enable the gradual disengagement of the main rotor and transfer power to the tail propeller. This system provides an effective means for power transfer to and from the main rotor to the tail rotor/propeller. In addition, this aircraft implements the use of fully rotational lifting surfaces which provide additional lift, anti-torque, and control authority. Through these innovations, the aircraft is capable of operating in forward flight at a significantly reduced power required. This reduction in power required correlates to a predicted increase in the aircraft's maximum velocity and range.

The Gyroblitz has been developed using a combination of trade studies, new ideas, revamped concepts, and borrowed ideas from completely different fields. The development process of the Gyroblitz has yielded successful ideas and effective combinations of concepts and configurations while also identifying ineffective and unrealistic ideas and concepts. The design of the Gyroblitz is able to successfully blend forward flight and hover systems into a single, efficient system. This Gyroblitz creates a path to enhance performance for future rotor designs.

Table of Contents

ACKNOWLEDGMENTS	I
EXECUTIVE SUMMARY	II
TABLE OF CONTENTS	III
LIST OF FIGURES	V
LIST OF TABLES	VII
1. INTRODUCTION	1
2. REQUIREMENTS ANALYSIS	1
2.1 DESIGN CRITERIA APPROACH.....	2
2.1.1 <i>Quality Function Deployment</i>	2
2.1.2 <i>Benchmark Helicopter</i>	3
2.2 OVERALL EVALUATION CRITERIA.....	4
2.3 OEC UTILIZATION.....	4
2.4 FINAL CONFIGURATION OEC RESULTS.....	5
3. CONCEPT DESIGN GENERATION AND EVOLUTION	6
3.1 VARIABLE ROTOR LENGTH/ RPM TRADE STUDY.....	7
3.2 FULLY ELECTRIC TRADE STUDY.....	9
3.3 AUTOGYRO CONFIGURATION.....	10
3.4 MULTI-PURPOSE CANARDS AND TAIL-LESS CONFIGURATION.....	11
3.5 ENCLOSED REAR FAN AND SIDE-SLOTS.....	11
3.6 CONTRA-ROTATING PROPELLERS AND A-TAIL CONFIGURATION.....	13
3.7 GYROBLITZ CONCEPT AND CONFIGURATION.....	13
4. VEHICLE PERFORMANCE	14
4.1 INTRODUCTION TO PERFORMANCE CALCULATIONS.....	14
4.2 CALCULATION TECHNIQUES.....	14
4.2.1 <i>System Modeling</i>	14
4.2.2 <i>Powered Rotor Power</i>	15
4.2.3 <i>Unpowered Rotor Power</i>	15
4.2.4 <i>Propeller Power</i>	15
4.2.5 <i>Canard and Wing Power</i>	15
4.2.6 <i>Parasite Power</i>	16
4.2.7 <i>Power Available</i>	16
4.3 CODE VALIDATION.....	17
4.4 PERFORMANCE ANALYSIS.....	18
4.5 IN-FLIGHT ROTOR TRANSITION MANEUVER.....	21
4.6 TRIM CALCULATIONS.....	22
5. DRIVE TRAIN	23
5.1 DRIVE TRAIN OPERATION.....	23

5.1.1 Engine transmission	24
5.1.2 Main Rotor transmission	25
5.1.3 Tail prop transmission	26
5.1.4 Tail Gearbox Control	28
5.1.5 Power Shaft	29
6. ROTOR DYNAMICS AND CONTROL	31
6.1 ROTOR CONTROL SYSTEM	31
6.1.1 Rotorcraft Control Schematics	31
6.1.2 Canard Control System - Canard Control Surface Operation	32
6.2 ROTOR DYNAMICS	34
6.3 ROTOR NOISE ANALYSIS	35
7. STRUCTURAL ANALYSIS	37
7.1 VEHICLE WEIGHT AND BALANCE	37
7.2 STRUCTURAL DESIGN CRITERIA	40
7.3 FUSELAGE DESIGN.....	40
7.4 LANDING GEAR DESIGN.....	41
7.5 VALIDATION/ANALYSIS	42
7.5.1 Tail Structure analysis	42
8. COST ANALYSIS.....	43
8.1 DEVELOPMENT COSTS	43
8.2 PRODUCTION COSTS.....	44
9. SAFETY AND CERTIFICATION	46
10. CONCLUSION.....	48

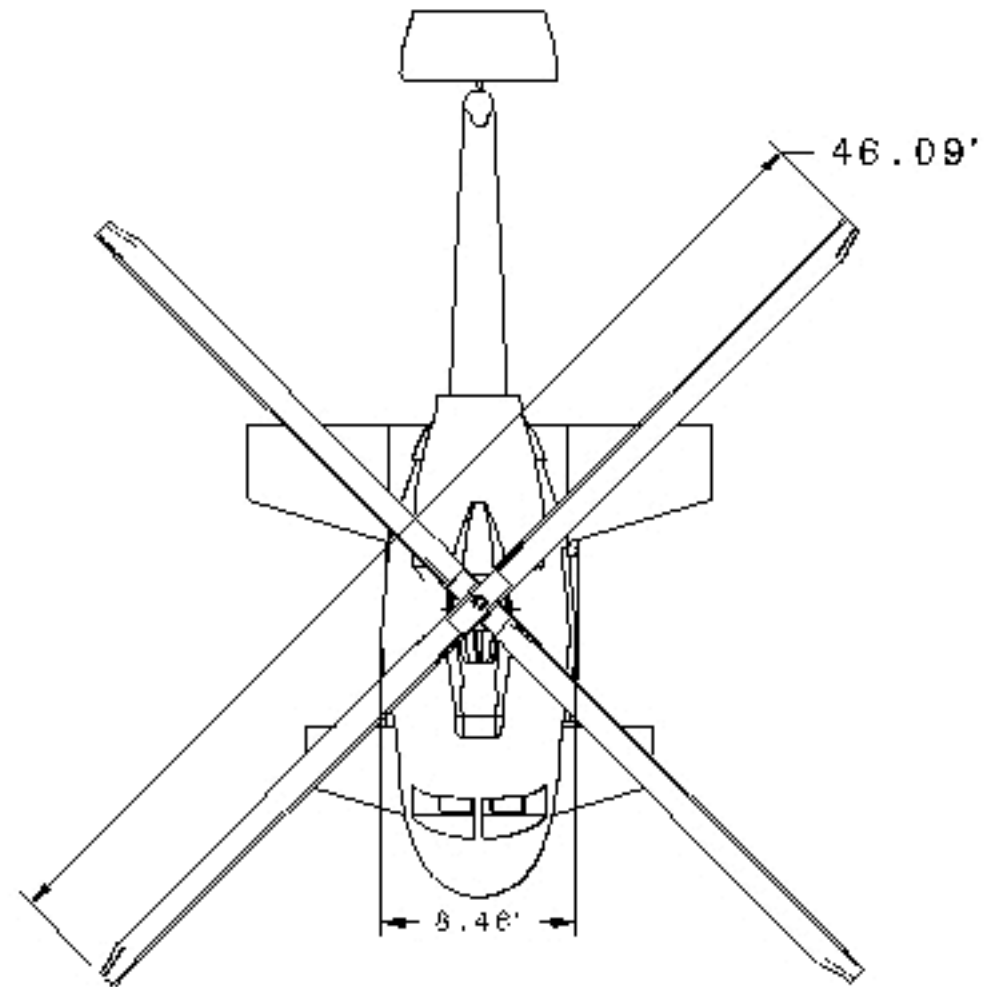
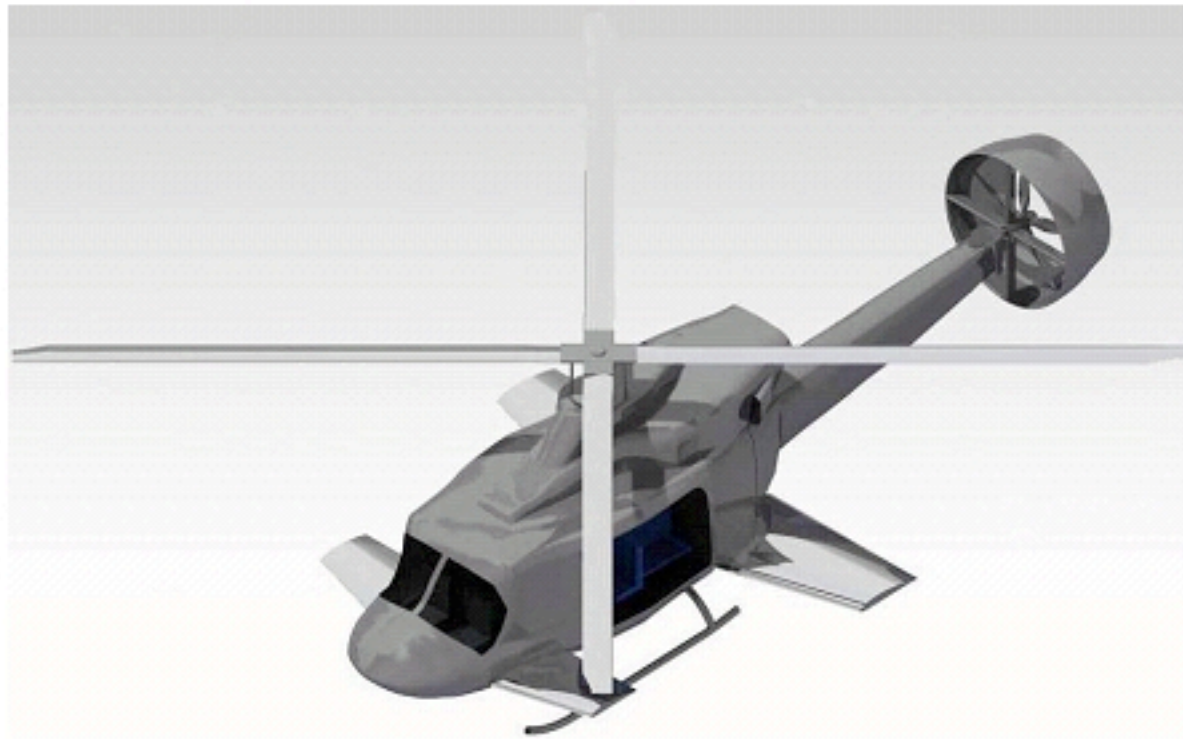
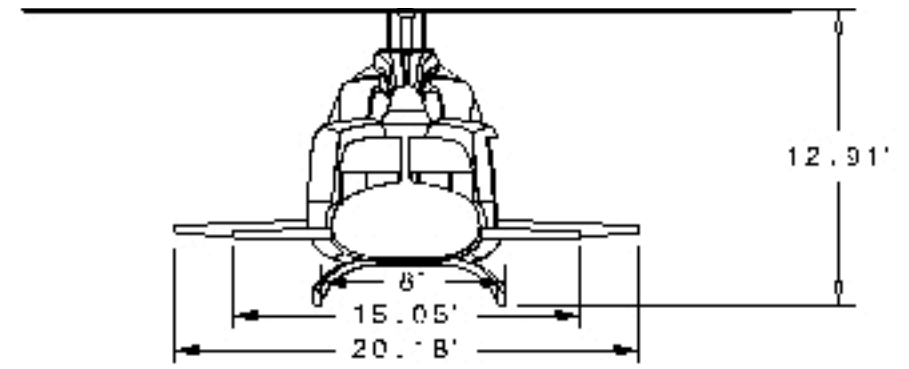
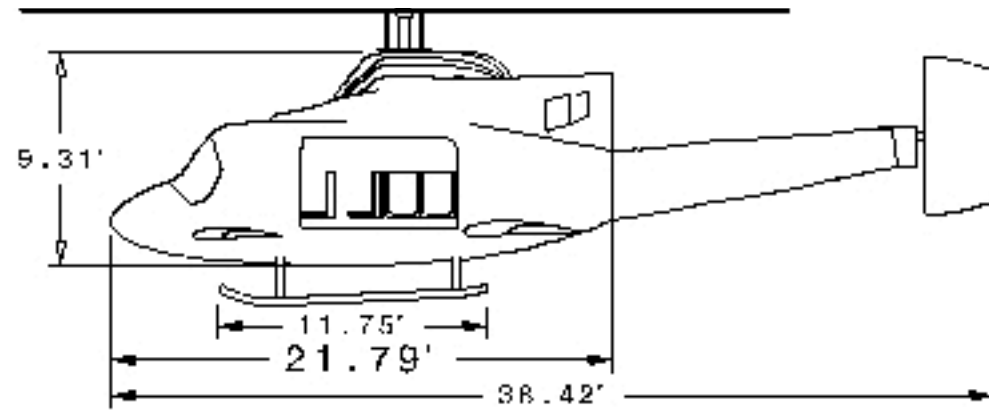
List of Figures

Figure 2.1. Performance Requirements	3
Figure 3.1. Concept evolution	6
Figure 3.2. Power Required versus Forward Flight Speed for various rotor speeds	8
Figure 3.3. Power Required versus Forward Flight Speed for various rotor radiuses.	9
Figure 3.4. Initial autogyro-helicopter hybrid rotor concept.....	10
Figure 3.5. Internal fan diagram.....	11
Figure 3.6. Encased fan configuration	12
Figure 3.7. Right: A-Tail configuration Left: Contra-rotating propeller configuration.....	13
Figure 4.1. Gyroblitz rotor state versus power and flight speed	16
Figure 4.2. Helicopter power required curve validation comparison.....	17
Figure 4.3. Autogyro power required curve validation comparison.....	18
Figure 4.4. Gyroblitz & Bell 412 Power Required, 10,000 Lb @ S/L	20
Figure 4.5. Maximum range comparison for Gyroblitz and Bell 412 at 5,000 ft.....	20
Figure 4.6. Maximum Velocity of Gyroblitz and Bell 412 at altitude and various gross weights .	21
Figure 5.1. Tail oriented to provide anti-torque	23
Figure 5.2. Tail oriented to provide forward thrust	24
Figure 5.3. Tail side-view, oriented for high-speed flight	24
Figure 5.4. Slip clutch system	25
Figure 5.5. Actively Controlled Slip Clutch.....	25
Figure 5.6. Two view of the Bell 412EP main-rotor transmission assembly	26
Figure 5.7. Two view of the tail gearbox	28
Figure 5.8. Shaft section of the power train for the Gyroblitz.....	29
Figure 5.9. Power train shaft connection	29
Figure 5.10. From left to right: C.V. joint, roller, and roller holder	31
Figure 6.1. Main rotor control scheme	32
Figure 6.2. Canard control surface diagram	33
Figure 6.3. Control surface pitch angle versus forward speed.	33
Figure 6.4. The spherical locations used for WOPWOP analysis.....	35
Figure 6.5. Graph of Pressure Levels calculated for 11,900 lbs gross weight.....	36
Figure 7.1. Gross Weight Center of Gravity Chart.....	39
Figure 7.2. Structural skeleton of the Bell 412EP	40

Figure 7.3. Gyroblitz tail structure.....	42
Figure 8.1. Development Cost Breakdown	43
Figure 8.2. Production Cost Breakdown Averaged Over 80 Units.....	44
Figure 8.3. Production Cost Breakdown Averaged Over 350 Units.....	45
Figure 8.4. Production Cost Summary by Type	46

List of Tables

Table 2.1 Comparative OEC values for various rotorcraft	4
Table 2.2. Gyroblitz OEC breakdown	5
Table 2.3. Gyroblitz OEC values	5
Table 4.1: Bell 412 Baseline Validation (11,900 Lb GW).....	18
Table 4.2. Gyroblitz Maximum Takeoff Weight Forward Flight Performance (11,900 Lb GW, 2,166 Lb Payload).....	19
Table 4.3: Gyroblitz Maximum Takeoff Weight Flight Performance (11,900 Lb GW, 2,166 Lb Payload)	19
Table 4.4: Gyroblitz Forward Flight Performance (10,000 Lb GW, 1,066 Lb Payload)	19
Table 4.5: Gyroblitz Flight Performance (10,000 Lb GW, 1,066 Lb Payload).....	19
Table 4.6. Gyroblitz dynamic trim results.....	23
Table 6.1. Canard control surface stepper motor functionality	34
Table 6.2. Sound levels for each case for both aircraft	36
Table 7.1. Weight model assembly for Bell 412EP and Gyroblitz	38
Table 8.1. Development Cost Summary	44
Table 8.2. Production & Unit Cost Comparison	45



|Scale 1:100 | GyroBlitz Three View Drawing |Dimensions in Feet|

1. Introduction

The American Helicopter Society states that the rotor/drive system is the core of the helicopter and recognizes that throughout the years countless versions of rotor/drive systems have been proposed and developed, but only a few of these versions have been taken into main stream operations. Manufactures and operators have only granted a limited amount of designs approval for large-scale production. The American Helicopter Society believes that with the advancement of design analysis techniques and the progress of material properties, a new non-conventional rotor/drive system can be proposed and developed to achieve the success shared by only a few other rotor/drive systems.

The competition calls for innovation of the conventional rotor/drive system configuration but with the end objective of being realistic not radical in order to provide a plausible alternative to the conventional rotor/drive system. The Gyroblitz is a realistic alternative to the conventional helicopter that successfully incorporates innovation, simplicity, and remarkable performance. This report describes the design process of the Gyroblitz outlining the conceptual evolution from the benchmark helicopter, performance methodology and analysis, drive train development and operation, analysis of the aircraft structure, control, cost, and safety.

2. Requirements Analysis

The AHS Student Design Competition's 2009 Request for Proposal (RFP) calls for the design of a new, nonconventional rotor/drive system for a helicopter, using as a starting point an existing design in terms of size, weight and performance. The RFP defines the rotor/drive system as the combination of rotors, rotor control systems, drivetrain and engines. The rotor/drive system is to endow the new design with improved performance in terms of speed, range, payload, endurance and noise signature.

The RFP specifies a series of guidelines and limitations to ensure feasibility of the design. These limitations include the inability to use physically impossible solutions such as:

- Materials endowed with exceptional mechanical characteristics that are not currently available ("Unobtainium" or composites so advanced and performing that no one has seen anything such yet).
- Engines or drivetrain with mechanical or thermal efficiencies not in line with the laws of thermodynamics and the manufacturing capabilities of current industry.
- Designs where functions are not clearly defined.

The RFP states that the final design should be capable of undergoing a certification process with an aviation authority and, therefore, should meet the requirements of a consistent set of certification rules. Additionally the design aircraft will retain all typical flight characteristics of rotorcraft, which are defined as the ability for hovering flight, flight in any direction, and the capability to perform power-off autorotation landings.

Additionally the RFP stresses innovation, and discourages relatively straightforward aircraft modifications such as outfitting a standard single main rotor-tail rotor configuration with a NOTAR or FENESTRON anti-torque device. Rather, new-truly innovative design ideas are sought.

Finally, the last requirement from the RFP is to choose a baseline helicopter with a MTOW over 3500Kg but not exceeding 5500 Kg, which filters the possible mission profiles for the design due to payload limitations.

2.1 Design Criteria Approach

Two main steps were taken to establish design criteria and clarify the RFP into pursuable goals. The first was to quantify the RFP's requirements; the second was to select a benchmark design. From these two steps the establishment of an overall evaluation criteria followed.

2.1.1 Quality Function Deployment

In order to quantify the RFP's requirements, a Quality function deployment (QFD) matrix was chosen to best translate the customer requirements into engineering requirements. Figure 2.1 shows the performance block (part of the engineering requirements) of the QFD. From this block, an importance on specifically improving the aircraft's speed was emphasized. Using the QFD, the RFP's specific call to increase endurance, range, cruise speed, maximum speed, and noise signature was directly translated to quantifiable engineering requirements. In addition, the request to innovate on the rotor/drive system was categorized into customer requirements from which a hierarchy was established to determine which areas of the rotor/drive system took prominence. As seen in Figure 2.1, the drivetrain was the most prominent feature to innovate on.

			Performance									
			Service Ceiling	HIGE Ceiling	HIGE Ceiling	Max Speed	Cruisespeed	MTOW	Range	Endurance	Cruise Altitude	
Direction of Improvement			↑	↑	↑	↑	↑	↑	↑	↑	↑	
WHATS	Performance	Improved Endurance	4.86%	0	0	0	1	9	9	1	9	3
		Improved Range	4.26%	1	0	0	1	9	9	9	3	9
		Improved Cruisespeed	5.32%	1	0	0	9	9	9	3	3	9
		Improved Max Speed	4.99%	1	0	0	9	3	9	0	1	3
		Noise Signature	2.34%	0	0	0	3	1	0	0	0	1
		Payload (people + cargo)	6.64%	3	9	9	9	3	9	9	3	1
	User	Aesthetics	2.13%	0	0	0	0	0	0	0	0	0
		Compactness	2.31%	0	0	0	1	1	9	3	3	0
		Easy to control	4.84%	0	0	0	3	1	3	0	0	0
		Reliability	6.63%	3	3	3	3	3	1	1	1	0
		Comfort	2.62%	1	1	0	3	9	0	0	0	1
	Survival	Damage Tolerance	4.02%	0	0	0	1	1	0	0	0	0
		Crash Tolerance	3.95%	3	3	3	3	3	1	0	0	3
		Environmental Tolerance	3.73%	0	0	0	0	0	3	0	0	3
	Cost	Affordability	5.05%	0	1	0	3	3	9	3	3	1
		Maintainability	4.82%	0	0	0	3	3	9	1	3	0
		Modular Design	5.83%	0	0	0	0	0	0	0	0	0
	Innovation	Engine	6.48%	9	9	9	9	9	9	9	9	9
		Drivetrain	7.18%	3	3	3	3	3	3	3	3	3
		Control Systems	4.27%	1	1	1	3	3	1	0	0	1
Rotors		5.65%	9	9	9	9	9	-20	9	9	9	
Misc.		2.10%	1	1	1	1	1	0	0	0	1	
Weighted Importance			2.06	2.36	2.28	4.04	4.09	3.52	2.83	2.71	2.92	
Relative Importance			2.28%	2.61%	2.53%	4.48%	4.53%	3.89%	3.13%	3.00%	3.24%	

Figure 2.1. Performance Requirements

2.1.2 Benchmark Helicopter

The selection of a benchmark was restricted to helicopters between 3500kg and 5000kg. At these weights, the description for all the candidate aircraft involved some form of medium utility aircraft. The Bell 412 EP was the chosen benchmark primarily due to the large knowledge base available for performance validation and comparison. The large amount of information available for the Bell 412 allowed for a greater understanding of the drivetrain and control systems. The Bell 412 is a versatile multiple role helicopter allowing for flexibility in mission selection for the final design.

2.2 Overall Evaluation Criteria

The main overall evaluation criteria formula for a rotorcraft design is as shown below.

$$OEC = \frac{33.22}{82.8} MiR + \frac{11.70}{82.8} SurR + \frac{9.87}{82.8} CoR + \frac{28.01}{82.8} RDSR$$

Each of the weights for the four individual ratings is determined through the relevant customer requirements and importance section seen in the QFD. The categories in the customer requirements directly tie into the survivability rating, cost rating, and rotor drive system rating. The mission rating ties both into the performance and user categories in the QFD.

2.3 OEC Utilization

In selecting a configuration, the OEC was utilized in determining which base configuration can yield the highest OEC value. Table 2.1 contains 6 actual aircraft and three conceptual configurations. The data for the actual aircraft was available but the data for the conceptual configurations had to be calculated. These three conceptual configurations represent, a single main rotor with separate electrical tail, a single main rotor in an auto-rotative state with a small tail, and an intermeshing autogyro with no tail. Some values for the three conceptual configurations had to be estimated in order to provide a comparison to the 6 actual aircraft. All estimates in performance for the three concepts were underestimated in order to account for inevitable problems. Using the OEC, preliminary analysis showed the autodyne (single main rotor in an auto-rotative state with a small tail) was the most preferable configuration.

Table 2.1 Comparative OEC values for various rotorcraft

Rotorcraft	OEC Value
Bell 412EP	0.86
Super Lynx 300	0.85
K-max 1200	0.82
AS365 Dauphin	0.86
S76 Spirit	0.82
Electric Tail (Conceptual)	0.89
Autodyne (Conceptual)	0.93
Intermeshing (Conceptual)	0.92

The OEC results show that the autodyne concept is the premier choice out of the 3 candidates.

2.4 Final Configuration OEC Results

Upon completion of the final design of the Gyroblitz, the final performance data was run through the OEC formula. Table 2.2 shows the final OEC value for the Gyroblitz. These values were obtained through the analysis techniques discussed in this report.

Table 2.2. Gyroblitz OEC breakdown

Parameter	Value	Target	Units	Parameter	Value	Target	Units
Interior Noise Level	90	81	dB	Auto-Rotation	1	1	
Exterior Noise Level	120	95.6	dB	Time Until Overhaul	900	1,250	Hrs
Cabin Space	220	220	Ft ³	Development	5	5	Years
Number of Seats	13	13		Unit Cost	6.7	5.8	Million \$
Pitch Control	14	14	%	Operating Cost	900	810	\$/hr
Roll Control	21	21	%	HOGE	2,400	3,000	Ft
Yaw Control	13	13	%	Cruise Velocity	155	143	Knots
Rate of Climb	1,300	1,350	Ft/min	Cruise Altitude	7,500	5,000	Ft
Fly by Wire	0.4	1		Max Weight	12,000	12,257	Lbs
Yield Airframe	400	400	MPa	Empty Weight	8,500	7,000	Lbs
Yield Rotor System	830	830	MPa	Range	508	442.2	nmiles
Max Cont. Hp	1,800	1,998	shp	Endurance	4	4.07	Hrs
OEI Max Cont. Hp	1,140	1,140	shp	SFC	0.6	0.5	lbs/Hp*hr

Table 2.3. Gyroblitz OEC values

Gyroblitz OEC Estimate	0.93
-------------------------------	-------------

From the OEC analysis, the Gyroblitz has a final value of 0.93. This value corresponds to an 8% increase compared to the benchmark Bell 412. That is to say, the Gyroblitz is effectively superior to the Bell 412 EP by 8% taking all things into account. The actual OEC value of the Gyroblitz is 0.930 and the autodyne archetype is 0.937. The Autodyne concept and the Gyroblitz have highly correlative OEC values that emphasize the well-aimed estimations made in the early part of design. The final design yielded higher than expected cruise speed and range, but lower payload and empty weight. Nonetheless, among all the 6 actual aircraft and conceptual configurations, the Gyroblitz has the highest OEC value.

3. Concept Design Generation and Evolution

The design of the Gyroblitz is a result of seeking innovation for the sake of performance contrast to seeking innovation for the sake of innovation. The Gyroblitz is the optimal result from a combination of new concepts, trade studies, and configuration variations. From the RFP analysis, innovation was greatly emphasized which called for the development of new concepts. The development of the Gyroblitz incorporated a wide variety of concepts ranging from new, original ideas to reviving old, inactive technologies to borrowing ideas from different fields. By expanding the concept base to such a wide range, the Gyroblitz was developed from an all-comprehensive foundation.

The final design of the Gyroblitz was a gradual process and involved thorough analysis of the implemented concepts and enough confidence in these concepts to progress further. Figure 3.1 shows the design progression from the benchmark Bell 412 to design of the Gyroblitz by a series of eight pictures. It incorporates basic core concept visualization (picture II) to modification (pictures II, III, and IV) to variation (V and VI) and eventually a combination of these archetypes to create the final product of the Gyroblitz.

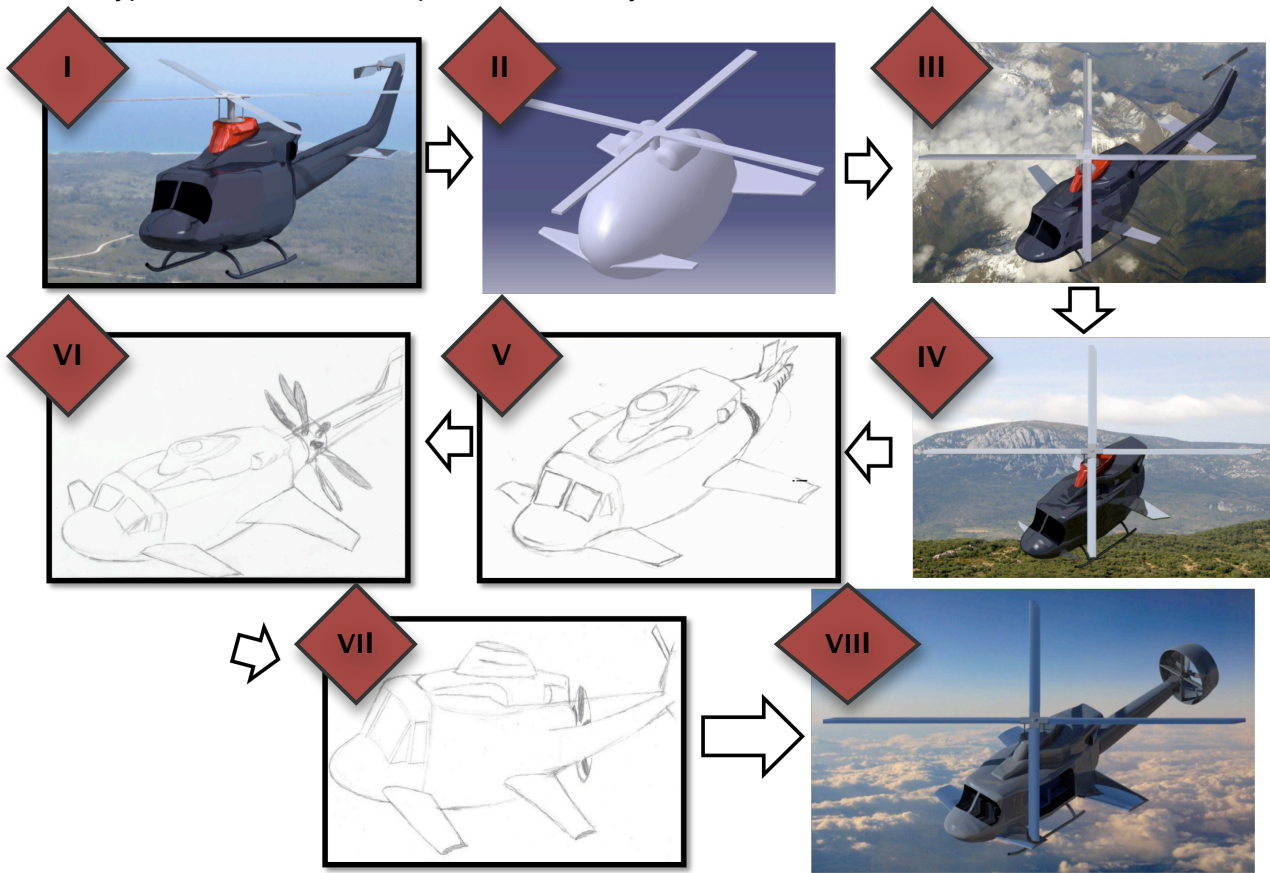


Figure 3.1. Concept evolution

3.1 Variable Rotor Length/ RPM Trade Study

In creating new and original concepts for the Gyroblitz, there existed two methods for advancement. The first was to take a concept, establish a means to implement it into the design, and obtain the final results from the modification. This method was not guaranteed to produce useful progressive results, as it was not always certain how the new and innovative ideas would affect the overall performance. The second, more preferable method was to calculate performance on varying a parameter of the rotorcraft in order to obtain the end results first. This method allowed for careful time investment, because if there was no notable increase in performance when varying a parameter, no further time would be devoted to that parameter. This next study highlights the advantages of the second method.

The RFP defines the rotor/drive system as the combination of rotors, rotor control systems, drivetrain and engines. Two prominent ideas that revolved around rotor modification involved a variable rotor radius length and variable rotor RPM condition. Before considering the structural adjustments or transmission modifications necessary to enable such ideas possible, a study was conducted on the end result of both of these parameters.

The conceptual advantages of having a variable RPM mechanism would allow for the flexibility of having a low power required and a low noise signature at low RPM's and being able to generate higher thrust at high RPM's. Using the blade element code discussed in section 5, various RPM values were input for the same gross weight of 7,000 lbs. Figure 3.2 shows various rotor speeds deviating from the baseline of 314 RPM set by the Bell 412 and employed by the Gyroblitz. It is evident that the rotor speed of 314 RPM is not always the ideal RPM to utilize for all forward flight speeds, but it should also be noted the amount of power reduction is small when comparing to other angular velocities. This study keeps all other parameters constant, including gross weight. The small advantage in power reduction would be obsolete when taking into account the weight of the mechanism used to allow for a variable RPM condition. In addition to adding transmission complexity, pushing for a variable rotor speed condition is not beneficial to a basic configuration in which the primary method of forward flight is in an auto-rotative state. Based on these conclusions, the idea of pursuing a variable RPM rotor was abandoned.

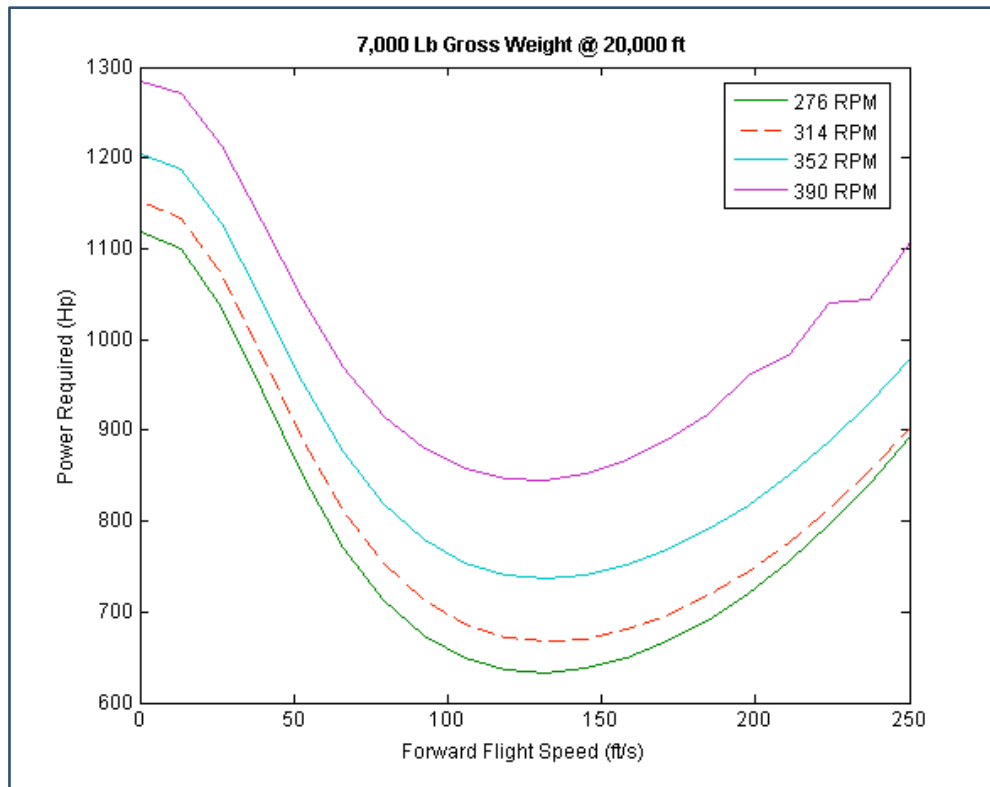


Figure 3.2. Power Required versus Forward Flight Speed for various rotor speeds

The other rotor concept was to create a rotor blade that can vary in length. This concept had similar reasoning as the variable RPM trade study. The shorter rotor radius corresponds to a reduction in noise as well as a decreased footprint and increased compactness, while a longer rotor radius corresponds to a larger thrust and generally lower power required.

The study was conducted using the same blade element code as the previous study. Figure 3.3 shows the results of power required versus forward flight speed with variable rotor radius. The Gyroblitz uses the same rotor radius, as the Bell 412 of 23 feet and, according to Figure 3.3, this is ideal for its dimensions. Decreasing or increasing the rotor radius is generally detrimental. Increasing the radius too greatly would prevent the rotorcraft from operating at higher velocities as indicated by the purple line (rotor radius of 31 feet).

Even if the results were slightly advantageous, the structural complexity of designing this feature is not very feasible and would involve some form of pin or joint that would negatively affect the rotor aerodynamics. Based on these conclusions, no further research regarding a variable rotor length was conducted.

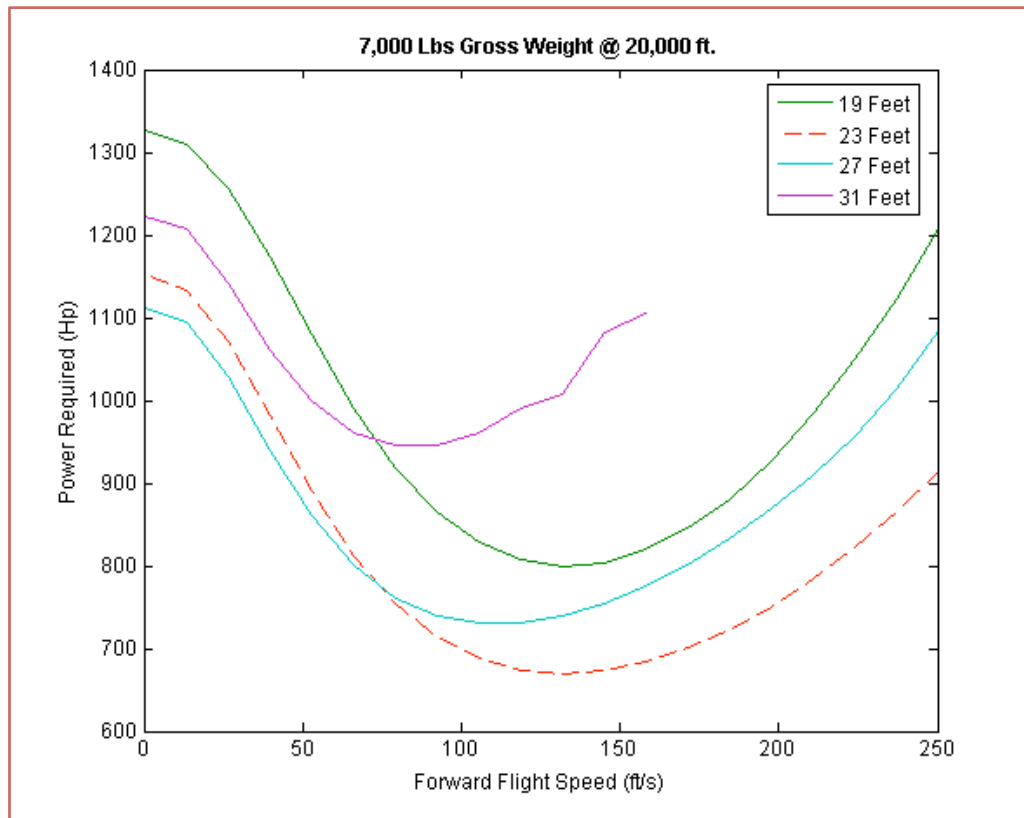


Figure 3.3. Power Required versus Forward Flight Speed for various rotor radiuses.

3.2 Fully Electric Trade Study

In borrowing ideas and concepts from other fields, there existed a strong desire to attempt to remodel the typical rotorcraft into a fully electrical powered aircraft. The advantages of having a battery-powered rotorcraft include a reduced weight and complexity with the reduction or elimination of a transmission, low maintenance required, and an eco-friendly aircraft independent of the fuel economy. A study was performed to gauge the required energy density for a mission profile involving two 15-minute hover conditions at sea level, two 90 minute cruise conditions at 10,000ft and a 30 minute hover at 5,000ft. This mission was analyzed using basic momentum-based disk actuator methods.

The study involved three gross weights of 7,000 lbs, 10,000 lbs and 11,900 lbs with a mission range of about 220 miles. For each gross weight, the mission profile was analyzed to determine the energy density (in watt hour per kilogram) required by the power source. Even for the lightest gross weight of 7,000 lbs, the energy density of such a mission was on average 1423 Wh/Kg (Watt-hours per kilogram). For a weight of 10,000 lbs the energy density required

was on average 2037 Wh/kg, and for the maximum gross weight of 11,900, the energy density required was on average 2476 Wh/kg.

Latest battery research suggesting that nano-particle $\text{Li}_4\text{Ti}_5\text{O}_{12}$ anodes could provide a revolutionary energy density of approximately 60 Wh/kg drove the investigation for a battery-powered rotorcraft. In order for a battery-powered, fully electric rotorcraft to be feasible, these batteries would have to provide an additional 3,700% energy density.

Completely replacing the main rotor/drive system with a battery and electric motor system was highly infeasible however, additional test were performed to see if an electric motorized tail rotor would be feasible and proved to be successful. Converting the current tail-rotor into an electrically powered tail rotor would greatly reduce the weight from the removal of the tail shaft and highly reduced tail reduction gearbox. This conclusion was kept as a reserve idea and was utilized in the A-tail configuration, which is discussed in section 3.6.

3.3 Autogyro Configuration

The idea to operate in forward flight in an autogyro condition originated from a concept outlined in Figure 3.2 below. This idea called for a turbojet or turbofan, during hover, to spin a vertical set of turbines, which would in turn spin the main rotor. In forward flight, the turbines would be disengaged and the engine exhaust would provide a forward flight thrust. This idea of having a disengaged main rotor in order for the engines to focus on forward flight thrust established the foundation of obtaining a faster flight speed for cruise and maximum speeds which has carried across to the final design of the Gyroblitz.

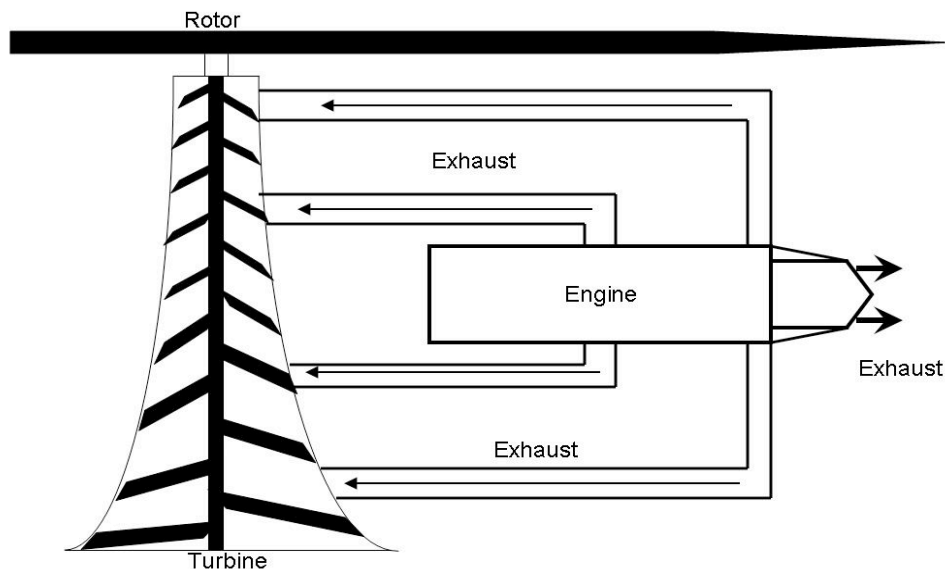


Figure 3.4. Initial autogyro-helicopter hybrid rotor concept

3.4 Multi-purpose Canards and Tail-less configuration

Early in the search for new ideas, the concept of having rotating canards, which could provide, in addition to additional lift, greater control authority and anti-torque became desirable. This idea proposed that a total of four canards in sets of two could deflect in an offset degree and completely provide the necessary anti-torque and enable the removal of the tail rotor entirely. The idea was an original concept and required analysis in terms of observing the effect of main rotor download interference, fuselage structural assembly to the canards, canard control, and most importantly sizing.

A preliminary estimate on the torque required to counter the main rotor came to be approximately 9000N. Using this value the surface area of the canards was estimated to be approximately 100 ft² per canard. Based on this estimation, the necessary anti-torque could not be provided by the canards alone.

3.5 Enclosed Rear Fan and Side-slits

In order to compensate for the large canard sizing, an idea to attach a rotating fan to the rear of the fuselage became desirable however due to the complex structural nature of having an external rotating fan so close to the fuselage, other suitable forms of rear thrust/anti-torque combinations were sought. One of the constructive alternatives called for an enclosed internal fan cased in a narrow shell as show in Figure 3.3. The idea was to have an opening for forward flight that could close and reveal a side set of slits to allow for the flow to turn and provide anti-torque.

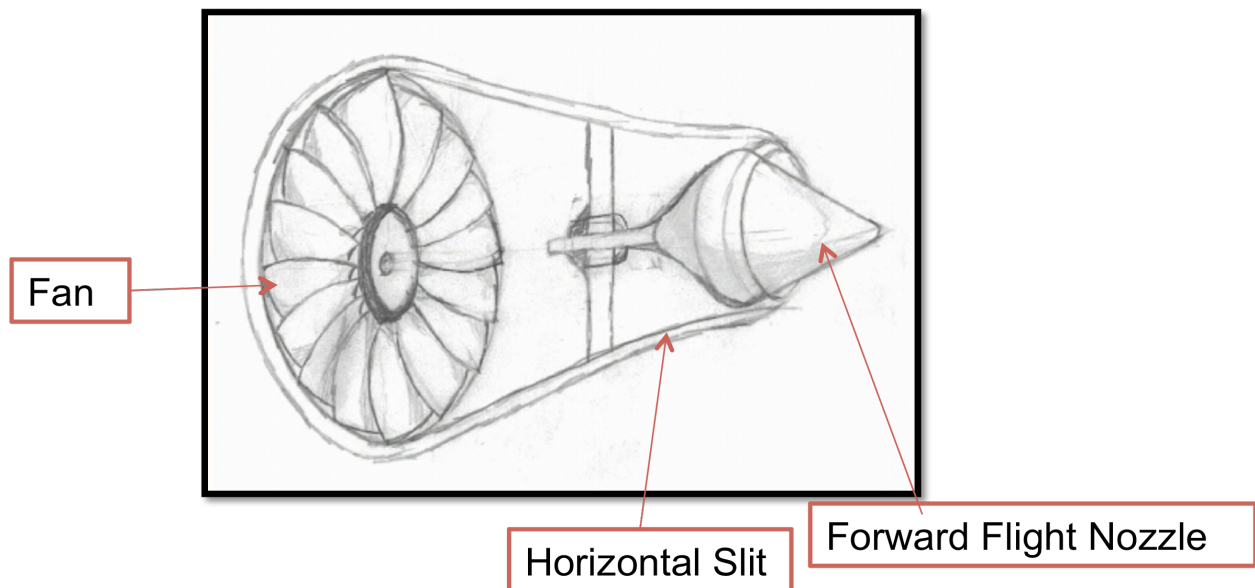


Figure 3.5. Internal fan diagram

This configuration would still allow for a highly innovative aircraft however at a significant cost in performance. Figure 3.4 shows the completed assembly for the enclosed fan configuration. The problems with the configuration included significant fuselage modification to feed flow to the rear fan, flow obstruction caused by the cork-like mechanism used to open and close the forward flight nozzle, loss in turning efficiency due to the flow not being smoothly guided to the horizontal slits. In addition, preliminary sizing was conducted for the radius of the fan and an estimated 3ft radius would be required at such a close location. In addition to an increased rotor download, the weight of the casing, nozzle, and linkages to control the nozzle and slit adds weight to the aircraft. From initial research on fan design, it is inefficient to have a single fan try to operate at two distinct operating angular velocities: one for forward flight and another for hover. Finally, the team's experience with fan performance was not as developed as the extensive work conducted with propeller performance. The severity of problems with the encased fan concept was too great to overlook and innovation for the sake of innovation at the cost of performance was not the direction chosen. The Main advantages with this configuration would be a very compact size, reduced complexity as a single system would be possible for both forward flight and hover, and aesthetics all factors which did not take precedence in the QFD weighted importance.

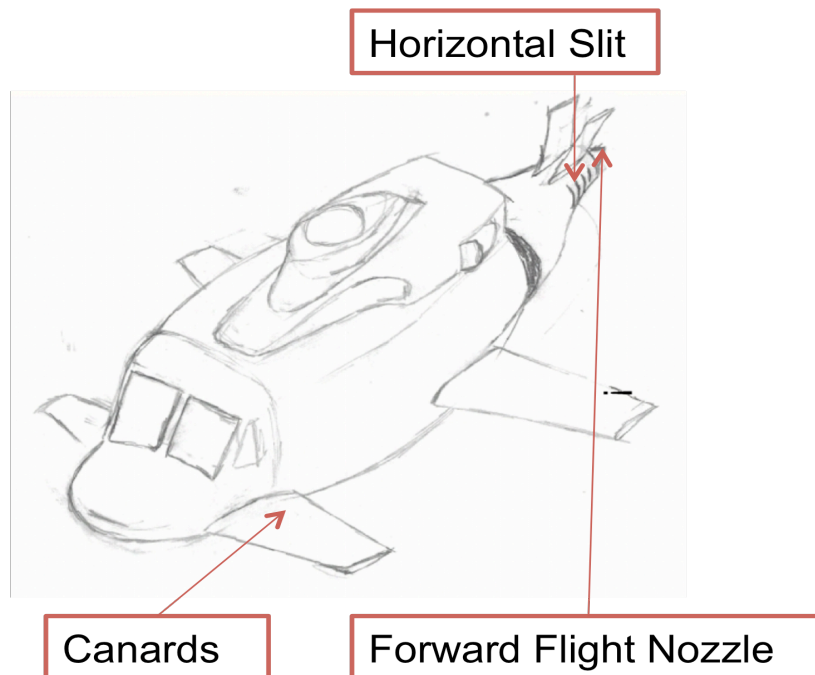


Figure 3.6. Encased fan configuration

3.6 Contra-Rotating Propellers and A-Tail Configuration

The idea of having a single system for both hover and forward flight was appealing but implausible at a location close to the fuselage. The need to re-establish a tail boom became apparent as any form of anti-torque fan or propeller close to the fuselage proved to be inadequate in generating the required anti-torque. Based on the results from the encased fan design, a conclusion was formed that it is inefficient to merge forward flight and hover systems. This conclusion was the approach for future configurations at least until the consideration of moving the propeller/fan to the end of the tail became available. Two configurations arose which incorporated separate systems for hover and forward flight. The first, utilizing a contra-rotating propeller configuration and NOTAR combination, proved to be profoundly complex and significantly heavy. Figure 3.5 shows the contra-rotating propeller configuration that utilized two separate sets of planetary gear systems to allow for the twin propeller configuration. The second configuration utilized a large propeller close to the fuselage as previously attempted by a fan but having an A-tail configuration with a tail rotor to provide for an anti-torque as shown in figure 3.5. The A-tail configuration would utilize an electric motor the tail rotor as the trade study demonstrated that an electrically powered tail rotor would be entirely feasible and practical for use. The A-tail configuration was a satisfactory configuration with the exception of obvious flow obstruction by the end of the tail. Other problems with the A-tail configuration included having to raise the landing gear in order to obtain sufficient clearance with the propellers location.

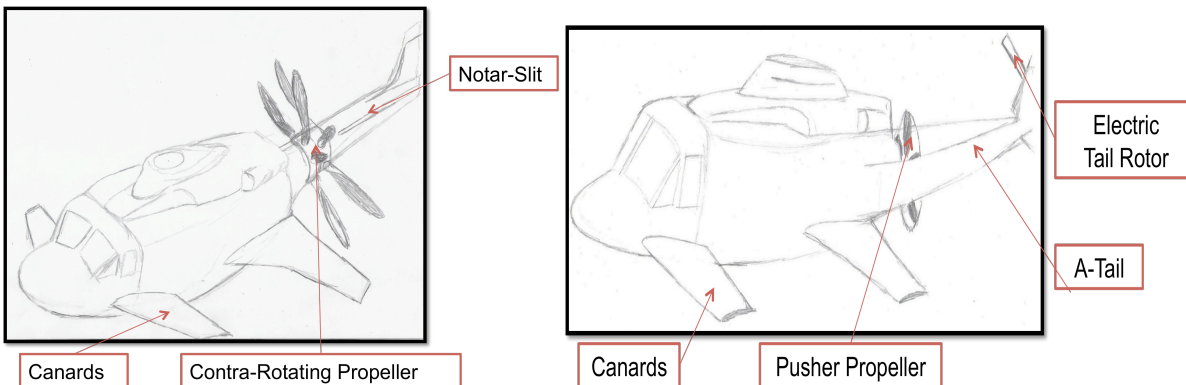


Figure 3.7. Right: A-Tail configuration Left: Contra-rotating propeller configuration

3.7 Gyroblitz concept and configuration

The final configuration for the Gyroblitz utilized the conclusions of all the previous iterations. The Gyroblitz is successful in evading the numerous difficulties with having a propeller/fan close to the fuselage; minimizing flow obstruction in propeller placement; avoiding fully encapsulating a fan/propeller. The final design was only possible with the simplicity of the gear system used to

rotate the propeller that is described in detail in Section 5. The Gyroblitz is truly successful in combining the forward flight and hover systems with minimal difficulty. With the design of the Gyroblitz, the original ideas of obtaining high speeds with autogyro capabilities were maintained.

4. Vehicle Performance

4.1 Introduction to Performance Calculations

The majority of the innovation injected into the Bell 412 focuses on increasing high-speed performance. Additionally, the operation of the vehicle in an autogyro state presents a radical change in the performance characteristics of the aircraft. For these two reasons, considerable importance has been placed on performance calculations in the design of the Gyroblitz.

Performance estimates for the Gyroblitz and the Bell 412 baseline were obtained using basic power analysis techniques. Range, endurance, max speed, ceiling, and climb rate were produced for various flight conditions through calculated values of vehicle power required and power available. Numerical solutions were obtained through MATLAB codes, which estimated rough trim conditions and accounted for the dynamic contributions of the main rotor, canards, wings, tail rotor, and propeller, were applicable.

4.2 Calculation Techniques

4.2.1 System Modeling

The first step in the development of the performance calculations consisted of modeling the Bell 412/Gyroblitz aerodynamic systems. The process of modeling the physical and dynamical behavior of the rotorcraft was based primarily on identifying the main rotor blade parameters such as blade radius, twist, chord, airfoil characteristics, and mass characteristics. Certain blade parameters were mathematically modeled so they could be used for better approximations in later blade element calculations. More specifically, great detail was placed on modeling the airfoil characteristics of the main rotor blade. The Bell 412 main rotor blade was found to have two airfoils best approximated by the Boeing VR-7 airfoil and the Wortmann FX-69-H083 supercritical airfoil. Using experimental data for these two airfoils, subroutines were written to compute the two-dimensional lift and drag coefficient for a given radial location along the main rotor blade. These subroutines used basic aerodynamic theory to estimate Mach compressibility effects, increased drag in transonic conditions, and lift and drag coefficients for off-design angles of attack. In addition to modeling the main rotor, detailed representations of the propeller and wing/canard system were produced to best approximate their behavior in-flight. Accurate rotor, propeller, and wing models were important in the computation of the rotorcraft

power required because they allowed for much greater confidence in the produced performance values.

4.2.2 Powered Rotor Power

The power required calculations were separated into two classes based on the state of the rotor for a given flight condition. The first class of power required calculations concerned the computation for the rotor in the normal working state. The code associated with this class of power calculations was used to compute both the Bell 412 baseline power and the Gyroblitz low-speed/hover power. Estimates for rotor torque, lift, and drag were calculated using blade element techniques in connection with uniform inflow calculated through momentum theory. Further rotor analysis converged on a rough trim condition to give steady level flight with the appropriate collective and cyclic control inputs. A separate blade element calculation was used to estimate the tail rotor power required for anti-torque.

4.2.3 Unpowered Rotor Power

The second class of power required calculations involved computation for the rotor in the windmill brake state. The rotor torque, lift and drag were calculated using blade element techniques with uniform inflow for the windmill brake state. Rotor disk angle of attack and collective pitch inputs were used to converge on a steady state, zero-torque trim condition with lift equal to weight.

4.2.4 Propeller Power

With the rotor thrust vector tilted rear for the autogyro state, the Gyroblitz required a separate source of thrust, supplied by a rear propeller, to offset the drag and rear component of the rotor thrust. The propeller power required was computed in the same manner as the powered rotor calculations. Blade element calculations were used to compute torque, thrust, and drag of the propeller while propeller collective input was used to converge on the desired thrust value.

4.2.5 Canard and Wing Power

The effects of the canards and wings on the vehicle performance depend on the configuration of the given lifting surfaces. When the lifting surfaces lie in the rotor wake for hover and sufficiently low speed forward flight, the surfaces are oriented at a given angle to the wake flow to reduce downloading and produce a small amount of the required anti-torque. When the surfaces are out of the rotor wake, they are oriented at a small angle to the freestream to produce lift and reduce the load on the rotor.

For the case of the lifting surfaces interacting with the rotor wake, the wake skew angle and contracted wake flow velocity were used to compute the drag, downloading, and torque produced by the lifting surfaces.

As the forward flight velocity is increased, first the canards and then the wings move out of the effects of the rotor wake. This can be seen in figure 4.1, a plot of the Gyroblitz power required outlining the different configurations of the lifting surfaces for varying forward flight speeds. For the case of the lifting surfaces lying outside of the rotor wake, the lift and drag are computed for a set small angle of attack to the freestream.

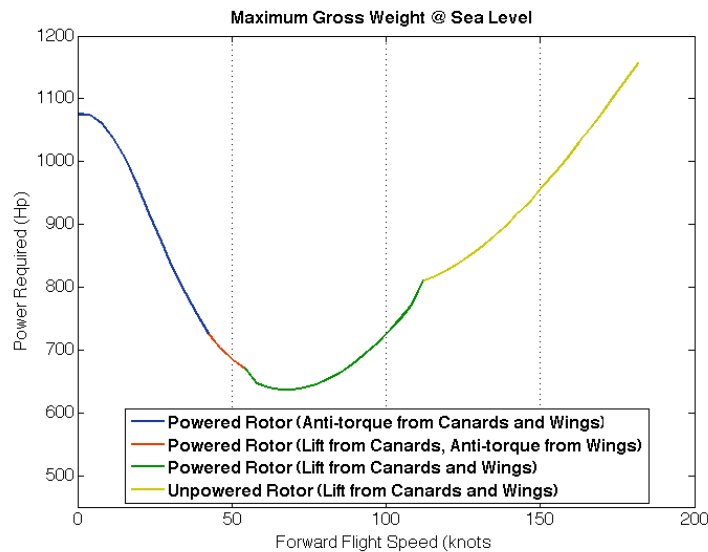


Figure 4.1. Gyroblitz rotor state versus power and flight speed

In the lifting surface calculations, the appropriate aerodynamic corrections were made for low aspect ratio wings. For simplicity, the induced drag was computed assuming elliptic lift distribution.

4.2.6 Parasite Power

Parasite power estimates were found using the approximate wetted frontal area of the bell 412 and a drag coefficient of 0.3. The same parasite power calculations were used for both the Bell 412 baseline and the Gyroblitz.

4.2.7 Power Available

It was assumed that the power supplied by the turboshaft engines was relatively constant with flight speed; therefore, no corrections were made for variations in engine output with flight

speed. Appropriate corrections were made for engine output with variation in altitude and atmospheric temperature.

4.3 Code Validation

The powered rotor codes were validated in several ways. First, simplifying assumptions were injected into the code and the final calculated values were compared to known closed-form solutions. This step allowed for the validation of the code calculations. Next, power required curves for the Bell 412 were produced and compared with similar curves supplied by an outside source and produced using Flightlab software. While these power curves did not match up exactly, they show the proper power behavior of the helicopter and the differences are due to dissimilarities in the system modeling of the bell 412. Figure 4.2 shows the power-required curves found using basic disk-actuator momentum theory and detailed blade element techniques, as well as the supplied Flightlab data.

The validation of the unpowered rotor code proved difficult; information and power data for an autogyro is limited, especially for the 5,000 Kg weight range. Power-required curves for the unpowered rotor were produced and compared with power curves for known fixed wing aircraft of similar weight to ensure the code was not grossly underestimating the power. Figure 4.3 shows the power-required curves for an autogyro found using blade element techniques and an approximate power curve for a Cessna Caravan 675.

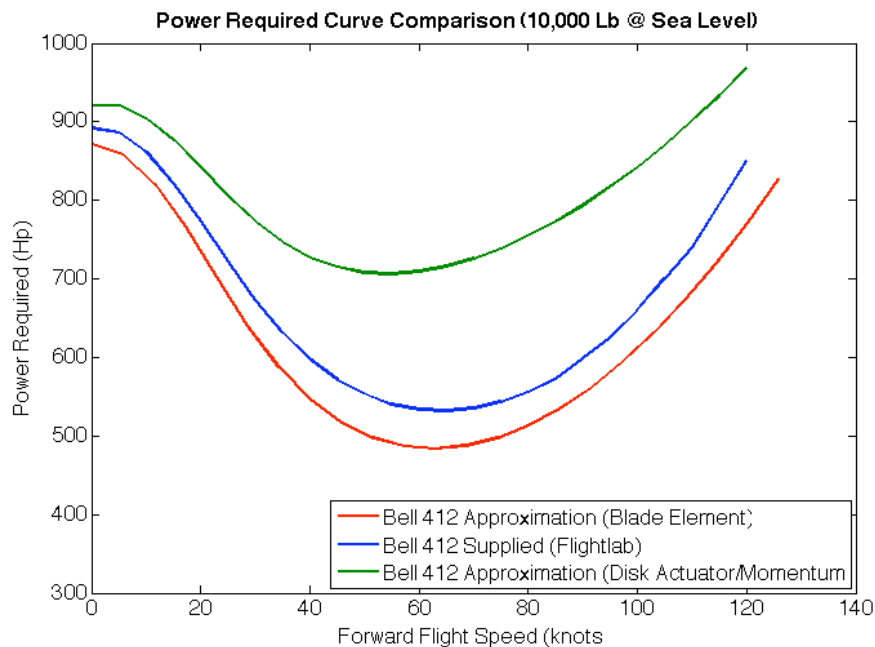


Figure 4.2. Helicopter power required curve validation comparison

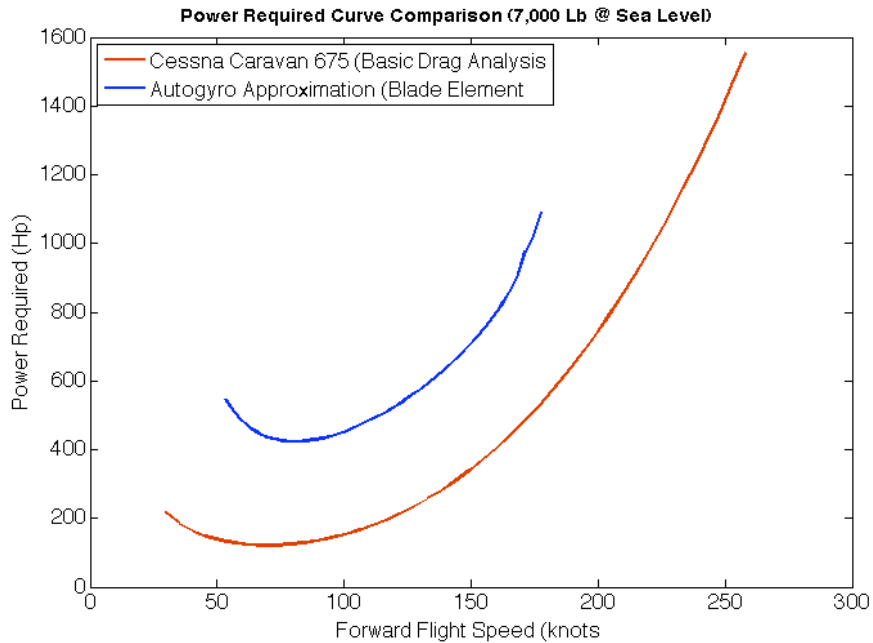


Figure 4.3. Autogyro power required curve validation comparison

4.4 Performance Analysis

Initial performance values were computed for the Bell 412 and compared with the posted values as another method of validating the codes. These values are shown in Table 4.1. While the values are not exactly the same, the error is within reason. Further comparative values for the Bell 412 are all computed using the blade element codes to give a more appropriate comparison of performance values.

Table 4.1: Bell 412 Baseline Validation (11,900 Lb GW)

	Predicted	Published	Error
Range Speed (5,000 ft)	141 kts	130 kts	8.5 %
Range (5,000 ft)	378 nm	402 nm	6 %
Endurance (S/L)	3.6 hrs	3.7 hrs	2.7 %
HOGE	5,400 ft.	5,200 ft.	3.9 %

Table 4.2 shows the estimated characteristic flight speeds for the maximum gross weight of the Gyroblitz at standard sea level and 5,000 ft altitude conditions. Furthermore, range and endurance estimates are shown for the same flight conditions in Table 4.3.

Table 4.2. Gyroblitz Maximum Takeoff Weight Forward Flight Performance (11,900 Lb GW, 2,166 Lb Payload)

Conditions	V _{Best Endurance} (Kts)	V _{Best Range} (Kts)	V _{Maximum} (Kts)
STD S/L	76	153	175
STD 5,000 Ft	82	160	168

Table 4.3: Gyroblitz Maximum Takeoff Weight Flight Performance (11,900 Lb GW, 2,166 Lb Payload)

	Value
Maximum Range (S/L)	410 nm
Maximum Endurance (S/L)	3.62 hrs
Maximum Range (5,000 ft)	419 nm
Maximum Endurance (5,000 ft)	3.6 hrs

With the increased empty weight of the Gyroblitz over the Bell 412, 10,000 lb gross weight represents a realistic medium-payload (w/fuel) takeoff weight; therefore additional performance metrics have been provided for this flight condition in Table 4.4 and Table 4.5.

Table 4.4: Gyroblitz Forward Flight Performance (10,000 Lb GW, 1,066 Lb Payload)

Conditions	V _{Best Endurance} (Kts)	V _{Best Range} (Kts)	V _{Maximum} (Kts)
STD S/L	63.7	161	183
STD 5,000 Ft	69.7	169	177

Table 4.5: Gyroblitz Flight Performance (10,000 Lb GW, 1,066 Lb Payload)

	Value
Maximum Range (S/L)	434 nm
Maximum Endurance (S/L)	3.92 hrs
Maximum Range (5,000 ft)	443 nm
Maximum Endurance (5,000 ft)	3.94 hrs

A comparison of the Bell 412 power curve and the Gyroblitz power curve in Figure 4.4 gives a proper visual representation of the increased performance of the Gyroblitz in forward flight. Operation in the autogyro-state allows for a noticeable drop in power required for speed above 95 knots. In Figure 4.4 the power trends are shown for the powered-rotor and unpowered-rotor modes at off-design flight speeds as the small dashed lines.

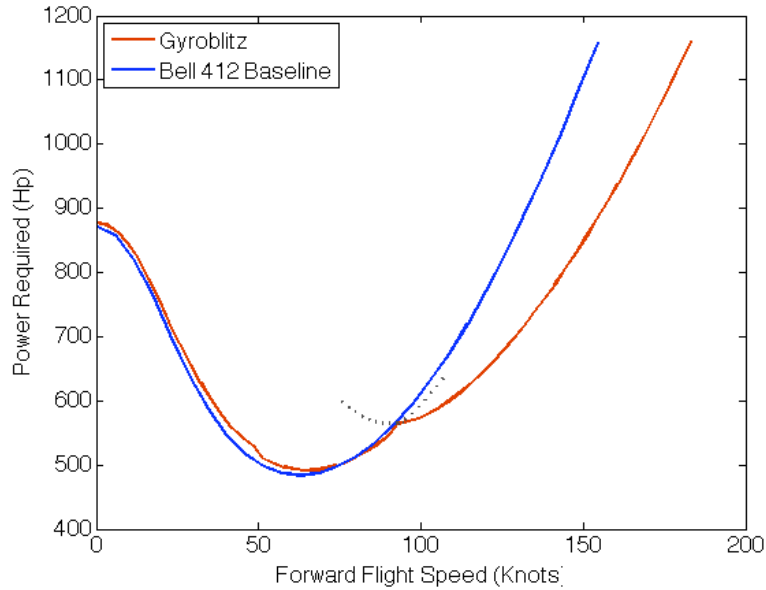


Figure 4.4. Gyroblitz & Bell 412 Power Required, 10,000 Lb @ S/L

The improvement in performance is seen specifically in the vehicle range and maximum velocity. Figure 4.5 shows the comparative increase in the maximum range of the Gyroblitz over the Bell 412 for various payload capacities at maximum fuel capacity. Figure 4.6 shows the comparative increase in vehicle maximum velocity with increasing altitude and for various gross weights. The autogyro maximum velocity drops below that of the Bell 412 for high altitude flight, however, this is beyond the normal operation altitude of the aircraft and are generally disregarded as a hindrance to the Gyroblitz performance.

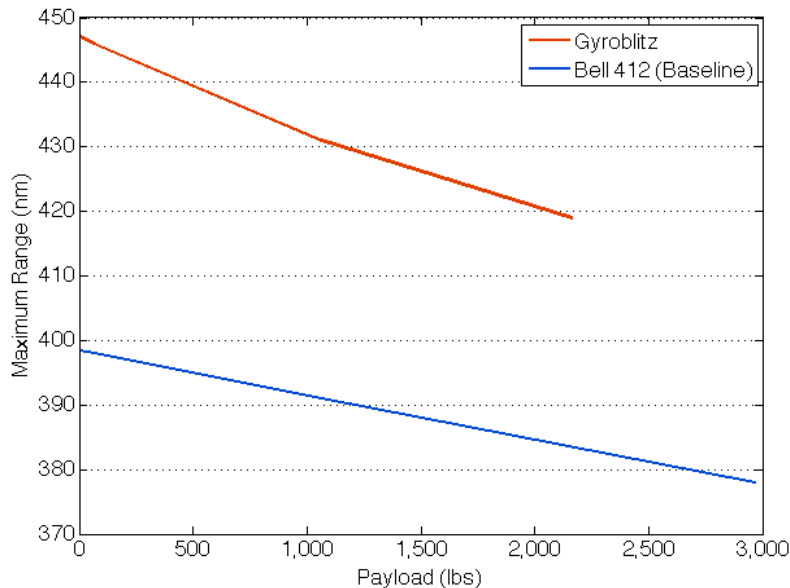


Figure 4.5. Maximum range comparison for Gyroblitz and Bell 412 at 5,000 ft

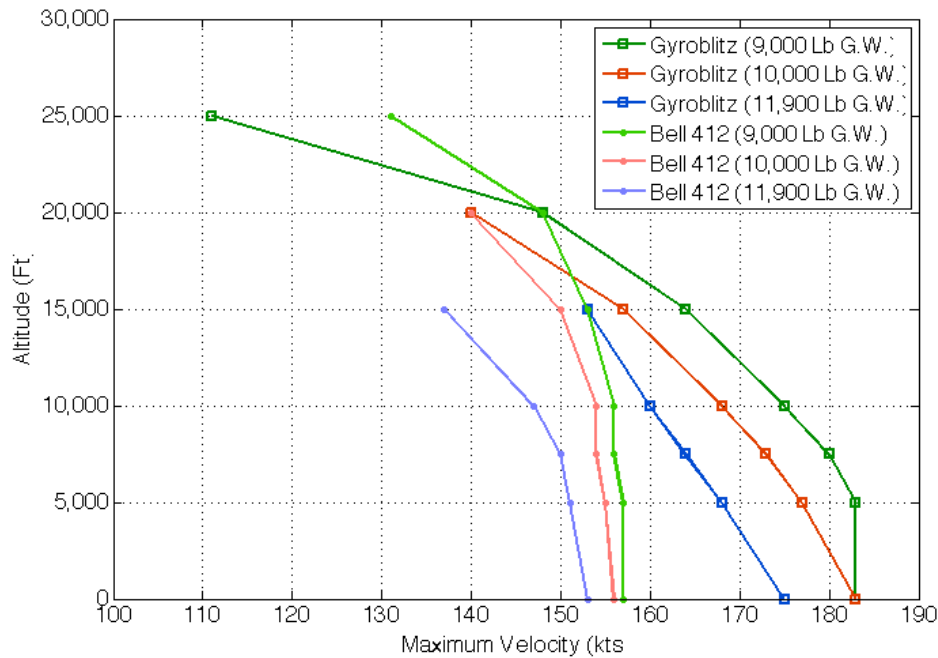


Figure 4.6. Maximum Velocity of Gyroblitz and Bell 412 at altitude and various gross weights

4.5 In-Flight Rotor Transition Maneuver

One of the key design advantages of the Gyroblitz is the ability to operate in a powered-rotor state for hover and slow speed forward flight, and the ability to operate in an auto-rotative state for high-speed forward flight. The transition maneuver required to enter the auto-rotative state is very important to the design. While this maneuver will require much more detailed analysis beyond the scope of this proposal, basic dynamical states and operational guidelines have been agreed upon.

To begin the transition maneuver from powered-rotor to auto-rotative rotor, the aircraft must attain the necessary forward flight speed that is sufficiently beyond the autogyro stall speed; the optimum transition speed correlates to the autogyro speed for minimum power required, around 100 knots. Additionally, the aircraft must be at an altitude of at least 5,000 feet, as this maneuver will result in a noticeable drop in altitude. At the proper flight conditions, the pilot will need to drop the collective pitch control and the engine power must be simultaneously redirected to the rear propeller assembly to reduce the overall torque on the main rotor. When power is cut to the main rotor, the pilot will have 2 seconds to drop the collective before the rotor decelerates to below 80 % of the normal operation levels. At this point, most of the rotor thrust is lost and the aircraft will begin to drop in altitude. Likewise, the flow will begin to change directions through the rotor as the rotor moves from the normal working state into the vortex-ring

state. Eventually the rotor will enter the windmill-brake state and the rotor will accelerate back to approximate normal operation level. Once in the windmill-brake state, control authority can be reestablished and the pilot will once again have full control of the vehicle.

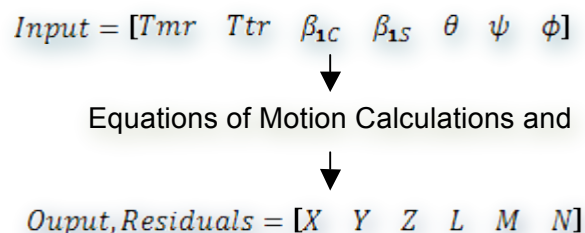
Assuming the aircraft enters a free fall during the transition period, initial estimates show that the Gyroblitz will reach a critical velocity of about 220 feet per second in about 7 seconds. Also assuming the transition maneuver requires up to 10 seconds to reestablish relatively steady-state flight, the initial estimates show a 1,350 foot drop in altitude.

The aircraft must also be capable of returning to a powered-rotor state for endurance flight, low-speed flight, hover, and landing. This maneuver will require the aircraft to return to the original transition flight condition of about 100 knots flight speed and at least 5,000 feet altitude. Collective and cyclic pitch controls must be dropped and engine power must be redirected back to the main rotor. As the rotor torque is increased the rotor will begin to change states and will eventually return to the normal-working state. Finally, steady-state flight will be reestablished through pilot control input.

In either maneuver, a failure to establish steady-state flight will force the pilot into an emergency auto-rotative landing.

4.6 Trim Calculations

The trim calculations for the Gyroblitz were carried out through a custom created program through MATLAB. The program is formulated to use an input vector of rotorcraft control characteristics and give an output of residual forces and moment in response to the inputs. The input and output vector is as such:



The trim calculations were performed in the states of the rotorcraft at close to empty weight and max weight and both at hover and a cruise forward flight speed of 150 knots. Two separate residual functions were created to analyze the different equations of motions due to the two distinct flight modes the Gyroblitz will experience. The method was to rigorously search for various input values to obtain an output vector of residual forces and moments with values of close to 0, thus trimming the rotorcraft. The results are shown in the following chart. Upon examining the results for trim condition, the take away from the results is that all the input values

needed are within the realm of capabilities in terms of engine and tail performance and also in terms of the various trim angles for the blades and the rotorcraft itself.

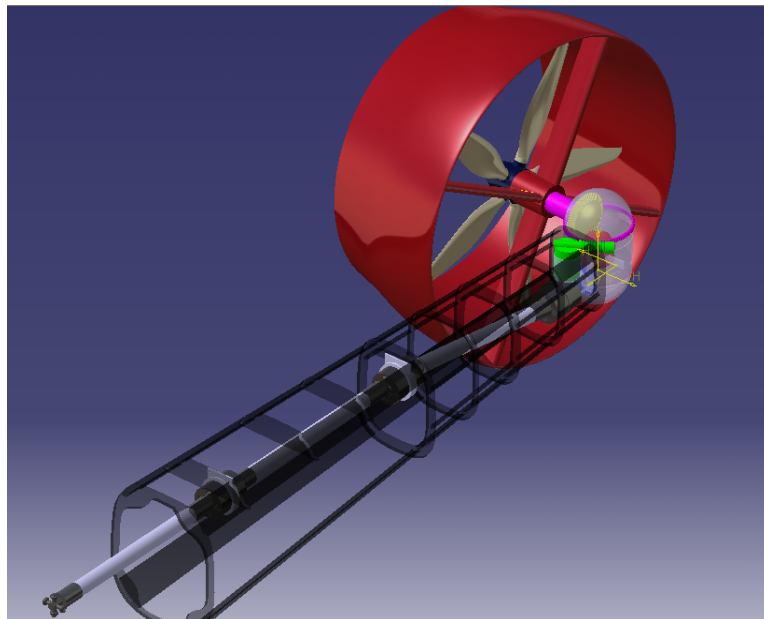
Table 4.6. Gyroblitz dynamic trim results

Trim Results	Weight (Lbf)	Main Rotor Thrust (Lbf)	Tail Rotor Thrust (Lbf)	B_{1C} (°)	B_{1S} (°)	ϑ (°)	Ψ (°)	ϕ (°)
Hover	7,800	7,805	432	3.33	-2.32	-3.33	0.00	0.86
	11,900	11,910	757	3.01	-2.69	-3.01	0.00	0.96
Forward Speed (250 knots)	7,800	5,080	670	-7.70	-0.92	-15.44	1.20	-0.79
	11,900	7,825	780	-2.23	-0.49	-13.44	1.22	-0.45

5. Drive Train

5.1 Drive train operation

The drive train consists of three different transmissions, two PT-6 engines, and several drive shafts. The primary concept of the Gyroblitz depends on the ability to move from powered hover to forward auto rotation seamlessly. To best understand the functionality is to break down the operation of the drive train system in modes of operation. The first is powered hover flight. In this mode the main rotor is powered through the slip clutch system that was added to the mast and the tail propeller is powered and set at a low

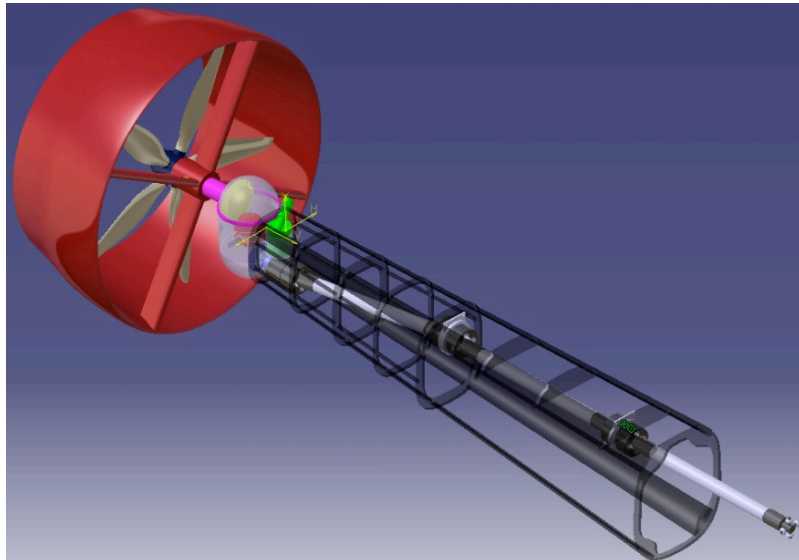


angle of attack. Moving from hover to vertical climb there is an increase or decrease to the propeller blade pitch to anti-torque the main rotor and for directional control through a hydraulic

Figure 5.1. Tail oriented to provide anti-torque

piston inside the propeller hub. Moving from hover to forward flight the tail propeller begins to rotate toward the forward flight position.

At the same time the main rotor is being unloaded by the canards the main rotor begins to



disengage through the slip clutch system and tilt the main rotor back in order to switch to auto rotation. Once the tail propeller reaches the forward flight position only the tail propeller is powered. For directional yaw control and stability control the propeller thrust can be vectored horizontally. The electric motor used to rotate the tail propeller is

Figure 5.2. Tail oriented to provide forward thrust

also used by the onboard computer to stabilize the aircraft.

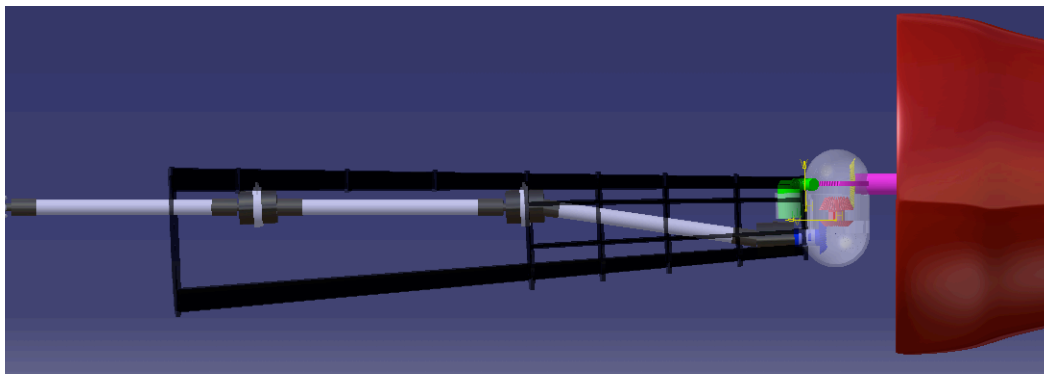


Figure 5.3. Tail side-view, oriented for high-speed flight

5.1.1 Engine transmission

The engine transmission in the Bell 412 is used to combine the power output of both the PT- 6 engines. The engine speed is reduced in this portion by 5:1 ratio and outputted at approximately 6600 RPM. The gearing for each engine contains a clutch, which engages only when torque is applied from the engine. This means that if the engine was to become disabled the clutch will automatically disconnect that engine from the power train. This gearbox also contains torque meter and torque controls to limit the power output of the engines such that both engines contribute to power output at all time.

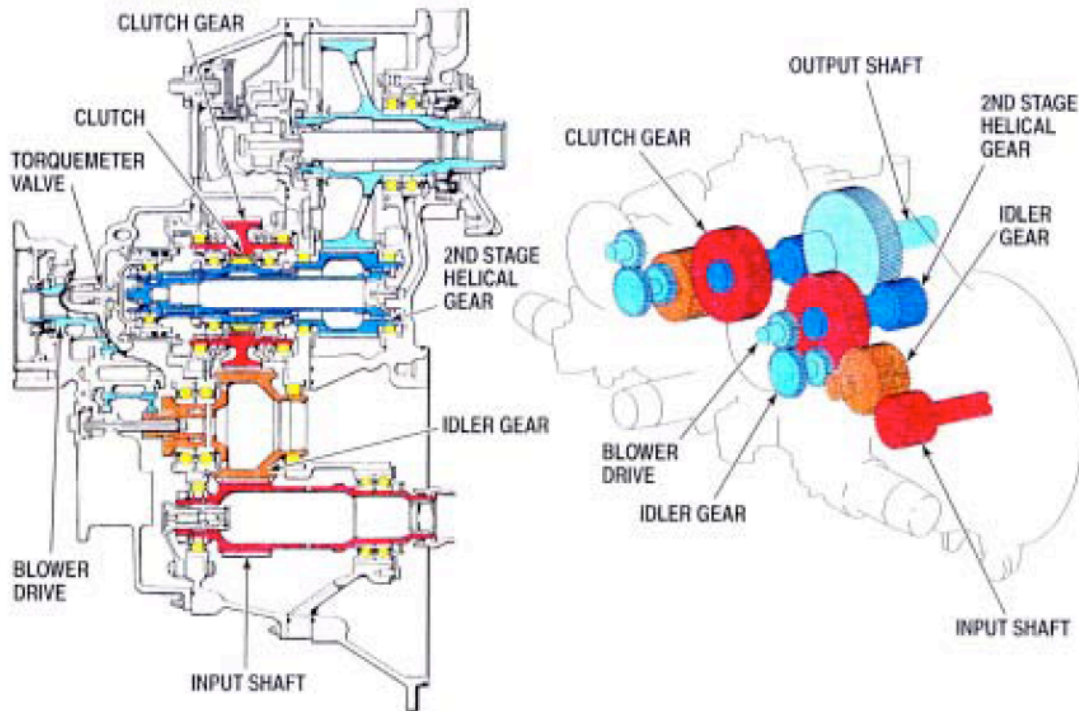


Figure 5.4. Slip clutch system

5.1.2 Main Rotor transmission

The Bell 412 main rotor transmission contains one input shaft and two output shafts, one for the mast and another for the tail. The design of the Gyroblitz converts the output to the tail to power the tail propeller used in the design. The mast output shaft rotates at 324 RPM and the tail output shaft rotates at 4200 RPM. In addition the main rotor transmission also provides power for the main hydraulic pump as well as several accessories. The main transmission uses a mast torque meter that measures the twist angle between the top and the bottom of the mast to determine the torque being applied to the main rotor. Once the torque limit is reached a warning is given to the pilot and if the torque continues to increase the engines are automatically trimmed.



Figure 5.5. Actively Controlled Slip Clutch

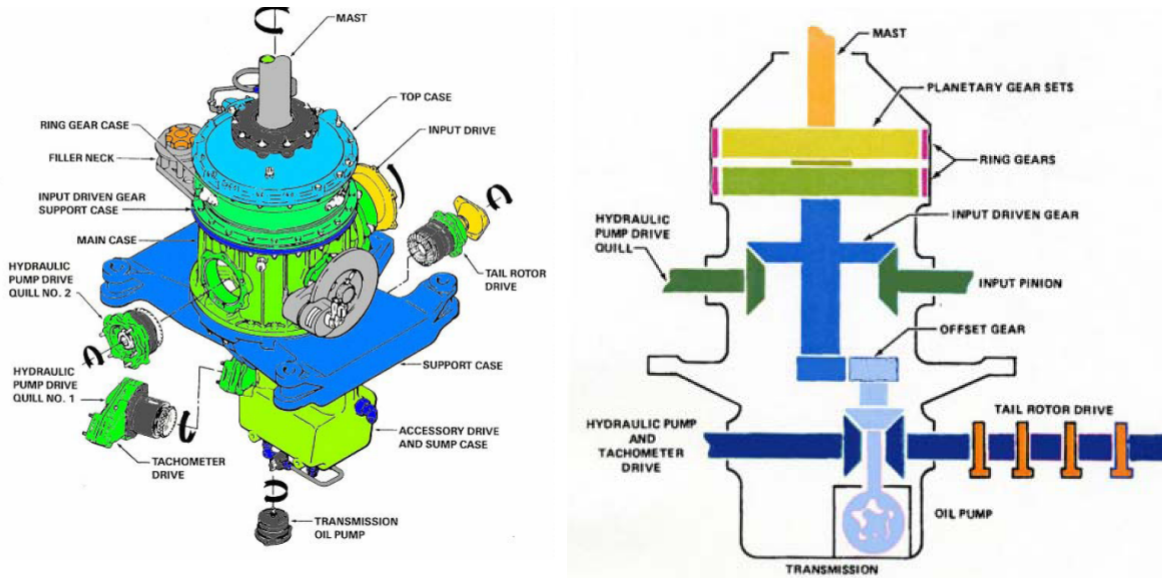


Figure 5.6. Two view of the Bell 412EP main-rotor transmission assembly

There are no significant changes in the construction of the main transmission. However there is the addition of an actively controlled slip clutch system to the tail and mast output shafts. This slip clutch system is used to manage the power output to the propeller and the main rotor. In addition it is used to disconnect the main rotor from the power train in forward flight and manage the power output to the tail.

5.1.3 Tail prop transmission

The transmission for the tail prop/fan consists of two sets of beveled gears at 90-degree angles. The first set of beveled gears has no gear reduction therefore both the gear and the pinion are identical. Both gears are beveled at 45 degrees with a face width of 1.8 inches. This value is one-third the cone distance. All gears were designed with a diametric pitch of 5. The pitch radius at the large end is 4 inches. The contact ratio was computed using the formula

$$m_p = \frac{Z}{P_c \cos(\varphi)}$$

where:

$$Z = \sqrt{(r_p + a_p)^2 - (r_p \cos(\varphi))^2} + \sqrt{(r_g + a_g)^2 - (r_g \cos(\varphi))^2} - C \sin(\varphi)$$

Since the pinion and gear are the same for the first part of the transmission the equation becomes

$$Z = \sqrt{(r_g + a_g)^2 - (r_g \cos(\varphi))^2} - C \sin(\varphi)$$

Solving for m_p ,

$$m_p = \frac{\sqrt{(r_g + a_g)^2 - (r_g \cos(\varphi))^2} - C \sin(\varphi)}{P_c \cos(\varphi)} = 1.71$$

To compute the power capacity of the gear system we used an empirical formula for power capacity for straight tooth beveled gears

$$H = \frac{S \times F \times V \times Y}{P \times 55 \times (600 \times V)} \times \frac{E - F}{E}$$

Where:

- S, the Static strength of material = 75000 Psi
- F, the face width = 1.7 in
- V, the pitch line velocity = 17592.92 ft/min
- Y, the Crown to cone center distance = 3.94 in
- P, the diametric pitch = 5
- E, the cone distance = 5.3 in

It is found that H = 1693 Hp

In the second set of beveled gears the rpm is reduced by 1.5:1 ratio. The drive gear is an 8-inch diameter at the large end and beveled at 33.7 degrees and pinion is a 12 in diameter at the large end. Both gears also have a diametric pitch of 5. First compute the gear meshing as above. It is found that $m_p = 1.75$ and then to compute the power capacity for the gear system it is found that

$$H = \frac{S \times F \times V \times Y}{P \times 55 \times (600 \times V)} \times \frac{E - F}{E}$$

Where:

- S, the static strength of material = 75000 Psi
- F, the face width = 2.4 in
- V, the pitch line velocity = 17593 ft/min
- Y, the crown to cone center distance = 1.41 in
- P, the diametric pitch = 5
- E, the cone distance = 7.21 in

It is found that H = 2484 Hp

Once both the proper meshing and power loading are verified the next step was to compute the other design criteria of the gears.

5.1.4 Tail Gearbox Control

The pinion rotates the tail propeller. Rotating the pinion around the axis of the idler gear controls the direction in which power is transferred through the gearbox. A worm and helical gear set carries out this rotation. In Figure 5.7, the pinion is seen attached to the helical gear through a bearing, which allows the pinion to rotate freely along its axis. The worm gear is operated by a reversible DC electrical motor. The reason a helical and worm gear set were chosen is because of their high gearing ratio that can be achieved for a relatively small gear. In addition, once the gears are at a specific position, they are automatically locked in place because of the high torque required for the spur gear to rotate the worm gear.

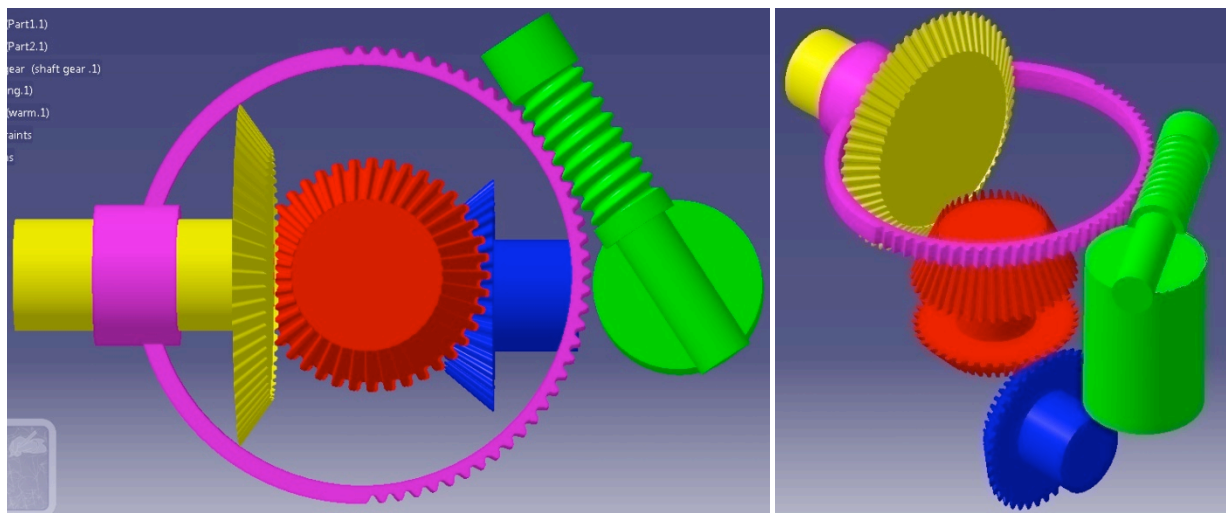


Figure 5.7. Two view of the tail gearbox

The helical gear is also attached to the gearbox, which is composed of two sections. The top section provides support for the helical gear and pinion and is attached to the bottom section via a groove and a v seal assembly. The bottom section supports the worm gear, idler gear, the input gear, and the input shaft and is attached to the tail structure.

5.1.5 Power Shaft

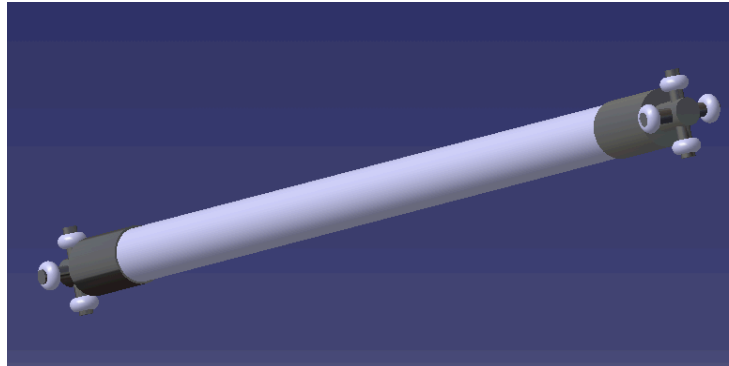


Figure 5.8. Shaft section of the power train for the Gyroblitz

In order to use the tail prop for both forward flight and as an anti-torque there is a need to be able to transmit the total power output of the engines to the propeller (1585 Hp). The first consideration to achieve this utilized a steel hollow shaft for this purpose. After doing an analysis on shaft sizing, it was found that the drive shaft will have to be about 9 inches in diameter and will weight approximately 900 lb. The weight of this shaft was unacceptable and other materials were considered, primarily carbon fiber for its very lightweight properties. The primary reason for avoiding carbon fiber is due to the expensive cost and difficulty of mass-producing. However, using the carbon fiber composite material the size of the shaft could be reduced to 1.85 inch for the outside diameter and an internal radius of .75 inch. To verify that the shaft is capable of transmitting the power available to the propeller a computation was performed to examine the maximum shear stress experienced by the shaft.

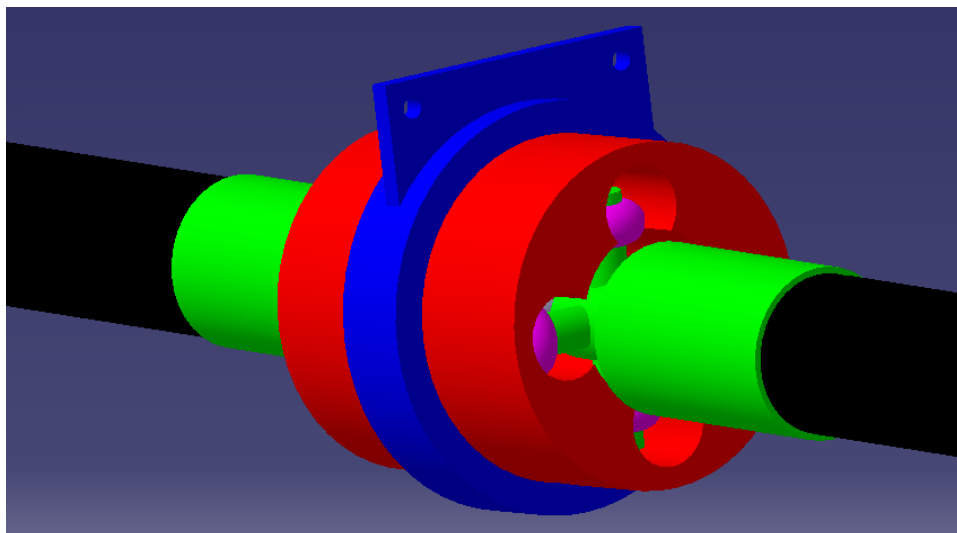


Figure 5.9. Power train shaft connection

The first step was to compute the torque at the shaft RPM (4200 RPM).

$$T = \frac{1585 \text{ Hp} \times 550}{\frac{4200 \text{ RPM}}{60} \times 2\pi} = 1982 \text{ ft} \cdot \text{lb}$$

Therefore, the maximum shear stress is

$$\tau_{\max} = \frac{1982 \text{ ft} \cdot \text{lb} \times \frac{1.85}{12}}{\frac{\pi}{2} \left(\left(\frac{1.85}{12} \right)^4 - \left(\frac{0.75}{12} \right)^4 \right)} = 353.9 \text{ ksi}$$

The maximum tensile strength of carbon fiber is 890 Ksi. The orientation of the fibers can be manually placed and for this shaft the fibers are placed in tension to achieve best performance.

To determine the length of the shaft, the critical speed to limit the shaft length is found.

$$L^2 = \frac{30\pi^2}{2\pi N_c} \sqrt{\frac{4gE(d_o^4 - d_i^4)}{64\rho(d_o^2 - d_i^2)}}$$

Where L is length of the shaft, E is the modulus of elasticity, N_c is the critical speed, and d_o and d_i are the outside and inside diameters, respectively.

$$L^2 = \frac{30\pi^2}{2\pi 4200} \sqrt{\frac{4(386.4)(22 \times 10^6)(3.7^4 - 1.5^4)}{64(0.065)(3.7^2 - 1.5^2)}} = 4049 \text{ in}^2$$

$$L_{\max} = 63.6 \text{ in}$$

The maximum length of the shaft can be over 63 inches but the Gyroblitz has a shaft length of 50 inches.

The shafts are connected to each other and to the gearboxes via a joint similar to a C.V. joint.

Each shaft has on both ends a titanium alloy roller carrier. The reason for using titanium alloy is serve as an inter face between the carbon fiber and the steel roller groves.

Since the carbon fiber composite and steel are electrically different materials they can setup a corrosive environment that will reduce the service life of the shaft assembly. In addition the titanium roller holder serves to dampen impact force absorbed by the shaft during power up. Each shaft carries four rollers at each end, which fit in four groves.

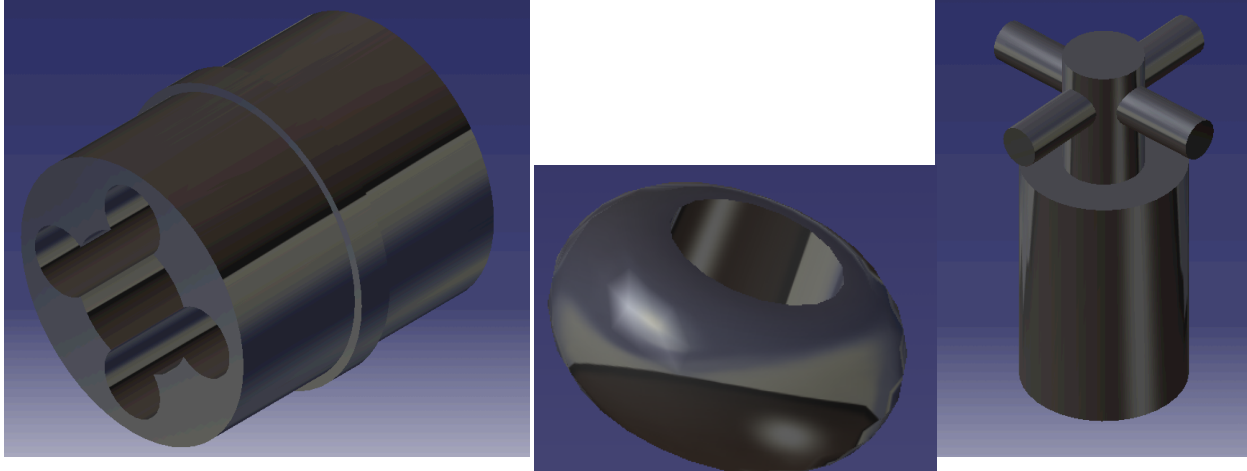


Figure 5.10. From left to right: C.V. joint, roller, and roller holder

The rollers are made of SAE 3042 steel this is hardened steel, which gives these rollers a longer service life.

The same steel is used for the roller grooves to minimize wear between the roller and the roller grooves. The roller grooves are attached carried by a bearing, which is attached to the frame. The C.V. joint is packed with grease to minimize friction between the rollers holder, the rollers, and the roller grooves.

6. Rotor Dynamics and Control

6.1 Rotor Control System

6.1.1 Rotorcraft Control Schematics

The main rotor control scheme will remain the same as the benchmark Bell 412EP. Figure 6.1 shows the links of the control stick to the actuators in the main rotor hub. The green colored connections correspond to the collective control system. The blue colored connections correspond to the cyclic control system.

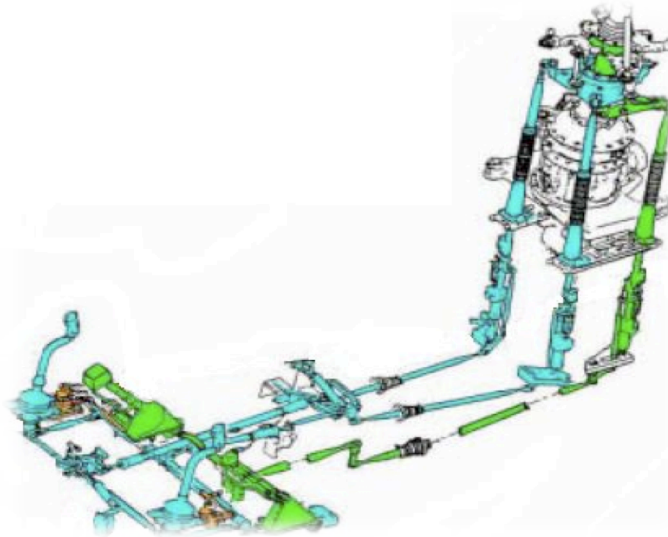


Figure 6.1. Main rotor control scheme

The controls of the control surfaces are operated through the flight stick and the strain gauges on the stick. The strain gauges allow the translation of pilot stick deflection direction and magnitude into electrical signals that is fed into the control surfaces' stepper motor circuitry units.

6.1.2 Canard Control System – Canard Control Surface Operation

6.1.2.1 Stepper Motor and Wire Selection

The sizing of the motor was determined with the consideration of the control surfaces' moments of inertia and their rotational angular acceleration of 0.1963 rad/sec^2 . This angular acceleration corresponds to having a control surface rotate from a pitch angle of 0° to 90° in 4 seconds. The stepper motor selected is the Anaheim Automation 34YSG Series Spur Gear Stepper Motor.

The wires connections feeding into the stepper motor are the power line and the 2 signal lines going into the circuitry unit. The total length for the 12 gauge 2.5 Amp wire power line is 26 ft. The 2 signal lines are small electrical lines that are assumed to have negligible mass.

6.1.2.2 Servo Motor Power Source

The stepper motors are power by the existing DC electrical system on the Bell 412EP. The existing DC electrical system is powered by two 30-volt, 200-ampere starter generator units, which in turn is powered though the engine's accessory gearbox. The stepper motor DC power will go through the dual buses in the DC control unit. Grounding is through the rotorcraft structure.

6.1.2.3 Control Surface Control Mechanism

The controls of the control surfaces are determined through 2 inputs into each servo's circuitry unit. The 2 inputs individually are the electrical signal from the pitot tube and its pressure transducer unit, the other input is the electrical signal from the strain transducer placed onto the pilot stick. The control scheme is shown in Figure 6.2.

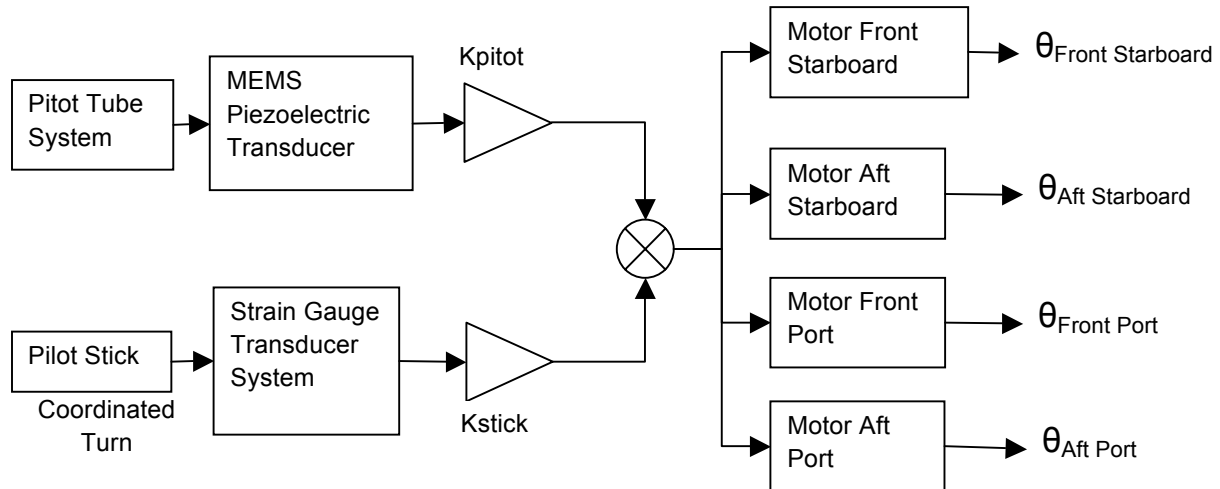


Figure 6.2. Canard control surface diagram

This control scheme is calibrated such that when the pilot stick is in neutral condition with no strain gauge readings, the only signal into the stepper motors are the forward speed electrical signal that will then determine the pitch angle of each control surface. The neutral stick scenario has a calibrated pitch angle with respect to speed as shown in Figure 6.3.

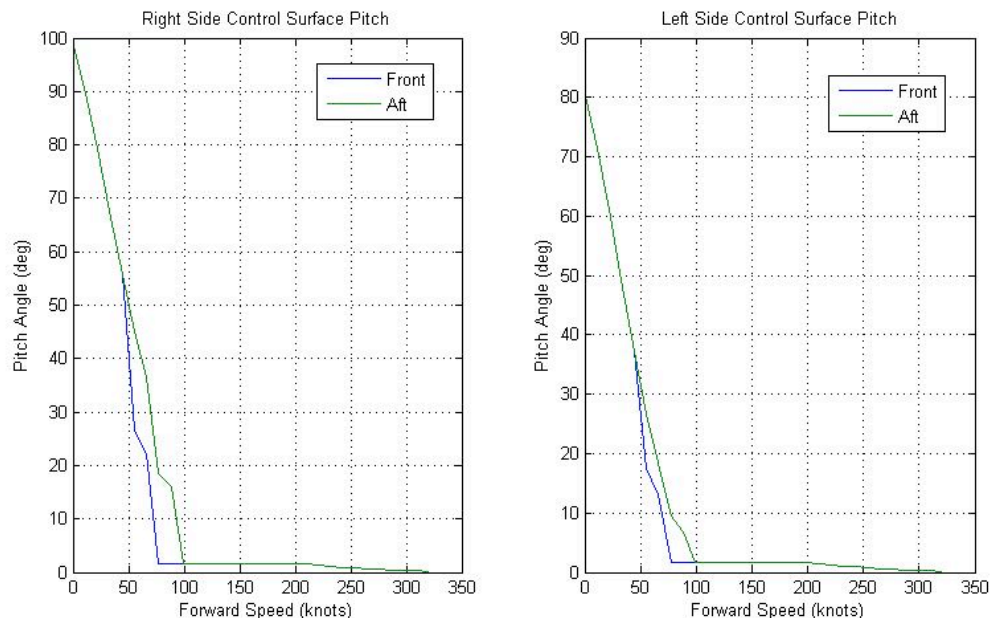


Figure 6.3. Control surface pitch angle versus forward speed.

The non-uniform regimes seen in the plots are due to the influence of the main rotor wake, the front control surface is out of the rotor wake region as the forward speed approaches 70 knots due to the decrease of the rotor wake skew angle, thus the front control surface will pitch close to the 0° position before the aft control surface. The relationship between the forward speed and voltage into the stepper motors is given by, where K is just the linear relationship between the two variables:

$$V_{motor\ input} (volts) = \frac{u_{forward\ speed} (knots)}{K (knots/volt)}$$

The operation of the pitch angle is not a continuous action suggested by Figure 6.3, but rather in steps. The stepper motor specifications will allow for 45+ steps from 0° to 90° pitch angle. Table 6.1 shows how each control surface stepper motor will operate. For the front right surface, for every increment of 1.7 knots in forward speed, the pitch angle of the control surface will pitch down 2°; when the control surface is out of the rotor wake influence it will have taken 45 steps into a 2° pitch angle.

Table 6.1. Canard control surface stepper motor functionality

Control Surface	Average Forward Speed Increment	Pitch Angle Increment	Steps Taken to Exit Wake
Front Right	1.7 knots	2°	45
Front Left	2.2 knots	2°	40
Aft Right	1.7 knots	2°	45
Aft Left	2.2 knots	2°	40

6.2 Rotor Dynamics

The Gyroblitz rotor blades and hub are designed to operate at a maximum of 324 rpm when at 100% torque in all flight regimes. This design is identical to the Bell 412 benchmark. The rotor blade assembly is a proven platform that when properly balanced avoids serious vibratory loading in both the hover and forward flight flying modes. Since the Gyroblitz operates in an auto-rotative state, the windmill speed of the rotors will not exceed the predesigned rotor rotational speed. At higher forward speeds, the rotor tip speed remains subsonic with sufficient altitude. When the Gyroblitz is in hover, the blades are spun at a maximum of 324 rpm to provide adequate lift. This produces no extra vibratory loading from the proven benchmark helicopter.

6.3 Rotor Noise Analysis

In accordance with the guidelines of the RFP, the noise signature of the rotor system was simulated, using the program WOPWOP. Simulation was also done for the benchmark aircraft and comparisons were made. It was determined to perform simulations for a combination of weights and forward velocities. The inputs needed to perform these simulations were generated using the performance code mentioned in section 4.

Using the code for each of the desired weight and velocity combinations, effective sectional lift

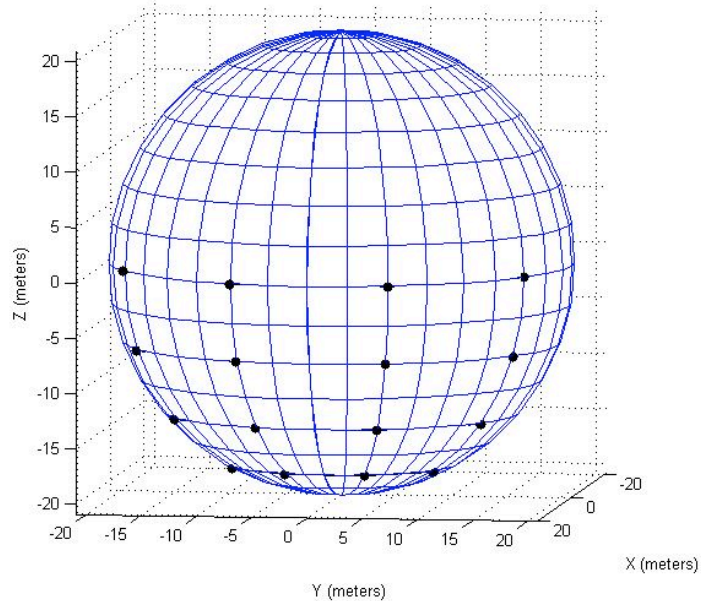


Figure 6.4. The spherical locations used for WOPWOP analysis

and drag coefficients, along with commanded inputs, were developed for a set of azimuthal and radial points on the rotor disk. Using this information, along with the characteristics of the rotor system, WOPWOP was able to generate sound pressure levels, in A-weighted decibels (dBA), for an observer located 21 meters forward of the aircraft. The program combined sound pressure from thickness and loading effects to get an overall sound pressure level created by the rotor system. WOPWOP produced pressure levels at 16 locations, located on a grid of points, each on a sphere with the observer distance as its radius and rotor hub as its center. The points of the grid are spaced evenly between locations 60 degrees to the left and right of the observer and zero to 60 degrees below. An example is seen in Figure 6.4. The black dots represent the points on the sphere that were used. For analysis of the sound levels seen for each flight condition, the 16 levels were averaged for each case and these values were compared.

The cases used had a range of weights, from 7,000 lb to the maximum gross weight of 11,900 lb. For each of these loads, a range of speeds from hover to 183 knots (maximum forward velocity) was used. Once performance data for each flight condition was found using the MATLAB code, the data was used in WOPWOP to determine the corresponding noise levels.

Table 6.2 shows the mean dBA values for each test. Each column corresponds to a forward flight velocity in knots, while each pair of rows corresponds to a gross weight.

Table 6.2. Sound levels for each case for both aircraft

Gross Weight/Vehicle		Hover	75 Knots	150 Knots	183 Knots
10,000 Lbs	Benchmark	72.7063 dBA	74.2405 dBA	82.0715 dBA	89.6221 dBA
	Gyroblitz	72.7063 dBA	74.2405 dBA	80.7166 dBA	89.4959 dBA
11,000 Lbs	Benchmark	72.7071 dBA	74.2418 dBA	82.0733 dBA	89.6207 dBA
	Gyroblitz	72.7071 dBA	74.2418 dBA	80.1529 dBA	88.9704 dBA
11,900 Lbs	Benchmark	72.7078 dBA	74.2430 dBA	82.0752 dBA	89.6196 dBA
	Gyroblitz	72.7078 dBA	74.2430 dBA	80.4714 dBA	88.8640 dBA

On investigating the charts, it becomes readily apparent that the difference in noise levels between aircraft is small. This is reasonable, as the rotor systems are similar. In fact, in low speed conditions, the two systems act in the same manner, leading to the identical noise levels at low speeds. As higher velocity is reached, the levels begin to show differences, often lower for the autogyro mode. A graphic representation of this is shown in Figure 6.5, which shows the values for the maximum weight cases. The lower levels for the Gyroblitz at higher speeds are due to the added lift of the canards, which reduces the load on the rotor.

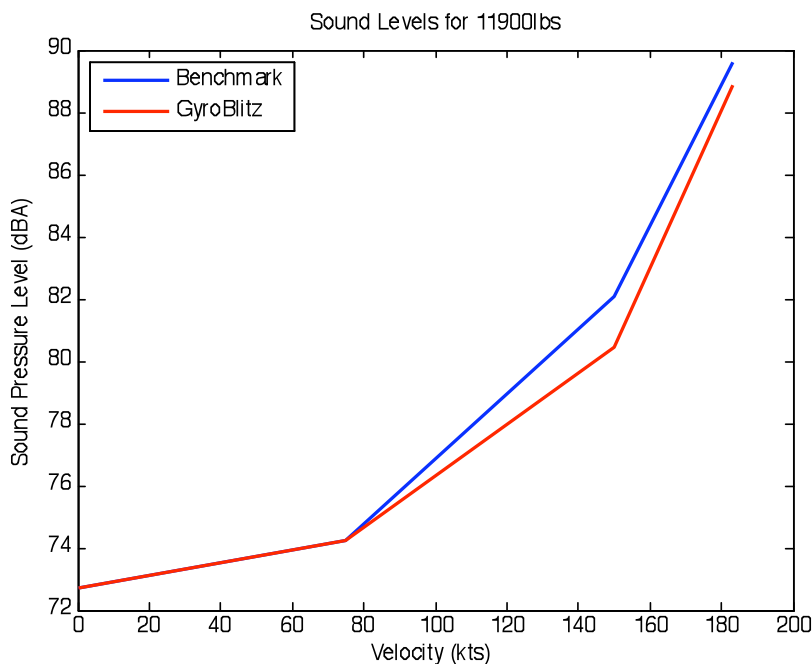


Figure 6.5. Graph of Pressure Levels calculated for 11,900 lbs gross weight

7. Structural Analysis

7.1 Vehicle Weight and Balance

In order to estimate the weight of the Gyroblitz and account for all of the new systems incorporated into the original benchmark a weight build up was performed. The weight build up was performed using both the Prouty weight estimation equations and known part weights for the Bell 412EP. The Prouty weight equations use the performance data from the helicopter as well as simplified geometry from the rotorcraft to predict the overall weight of designated main assemblies. Both the geometrical and performance data were gathered from the Bell 412EP flight manual and used to construct the weight model. The weight model was constructed and the benchmark was used for validation. In Table 7.1 below the weight model assembly breakdown for the Bell412EP is shown.

Table 7.1. Weight model assembly for Bell 412EP and Gyroblitz

Bell 412EP		Gyroblitz	
Component	Weight (Lbs)	Component	Weight (Lbs)
Main Rotor Blades	408	Main Rotor Blades	408
Main Rotor Hub and Hinge	228	Main Rotor Hub and Hinge	228
Stabilizer (horizontal)	50	Tail Rotor	385
Fin (Vertical Stabilizer)	61	Forward Canards (2)	77
Tail Rotor	38	Aft Canards (2)	162
Furnishings and Equipment	325	Furnishings and Equipment	325
Air Cond. & Anti Ice	95	Air Cond. & Anti Ice	95
Fuselage	665	Fuselage	927
Landing Gear	210	Landing Gear	210
Nacelles	51	Nacelles	51
Engine Installation	1,400	Engine Installation	1,400
Propulsion Subsystem	248	Propulsion Subsystem	248
Fuel System	146	Fuel System	146
Drive System	405	Drive System	545
Cockpit Controls	31	Cockpit Controls	31
System Controls	98	System Controls	108
Auxiliary Power Plant	150	Auxiliary Power Plant	150
Instruments	88	Instruments	88
Hydraulics	66	Hydraulics	66
Electrical	274	Electrical	314
Avionics	400	Avionics	400
Crew Doors	40	Crew Doors	40
Sliding Doors	90	Sliding Doors	90
Hinged Tail Panel	20	Hinged Tail Panel	20
Crew Seats	100	Crew Seats	100
Standard Seating	210	Standard Seating	210
Standard Interior Trim	166	Standard Interior Trim	166
Fire Extinguisher Gas	4	Fire Extinguisher Gas	4
Steps	28	Steps	28
Equipment	31	Equipment	31
Heated Windshield	10	Heated Windshield	10
ICS	8	ICS	8
IFR	103	IFR	103
Controls	93	Controls	93
Systems	150	Systems	150
Indicators	224	Indicators	224
Panel	6	Panel	6
Miscellaneous	5	Miscellaneous	5
Estimated Empty Weight	6724	Estimated Empty Weight	7651
Actual Empty Weight	6773	Empty Weight Increase	878
Percent Difference	0.7%		

The validation of the weight model shows a minimal percent difference in the empty weight of the Bell 412EP of less than 1%. With the model validated the weight build up was generated for the Gyroblitz. With the addition of the new components and systems to the weight model the total rotorcraft empty weight increased to 7651 lbs. This new empty weight is an increase of 878 lbs over the initial benchmark.

With the Gyroblitz empty weight calculated the next step was to ensure the center of gravity of the aircraft was maintained in order to achieve the Bell 412EP's normal flight characteristics. To achieve balance the tail boom was shortened and some of the subsystems were relocated in the aircraft sub floor forward of the rotor mast. The center of gravity station was then calculated at each gross weight. The results of the calculations are plotted below in Figure 7.2.

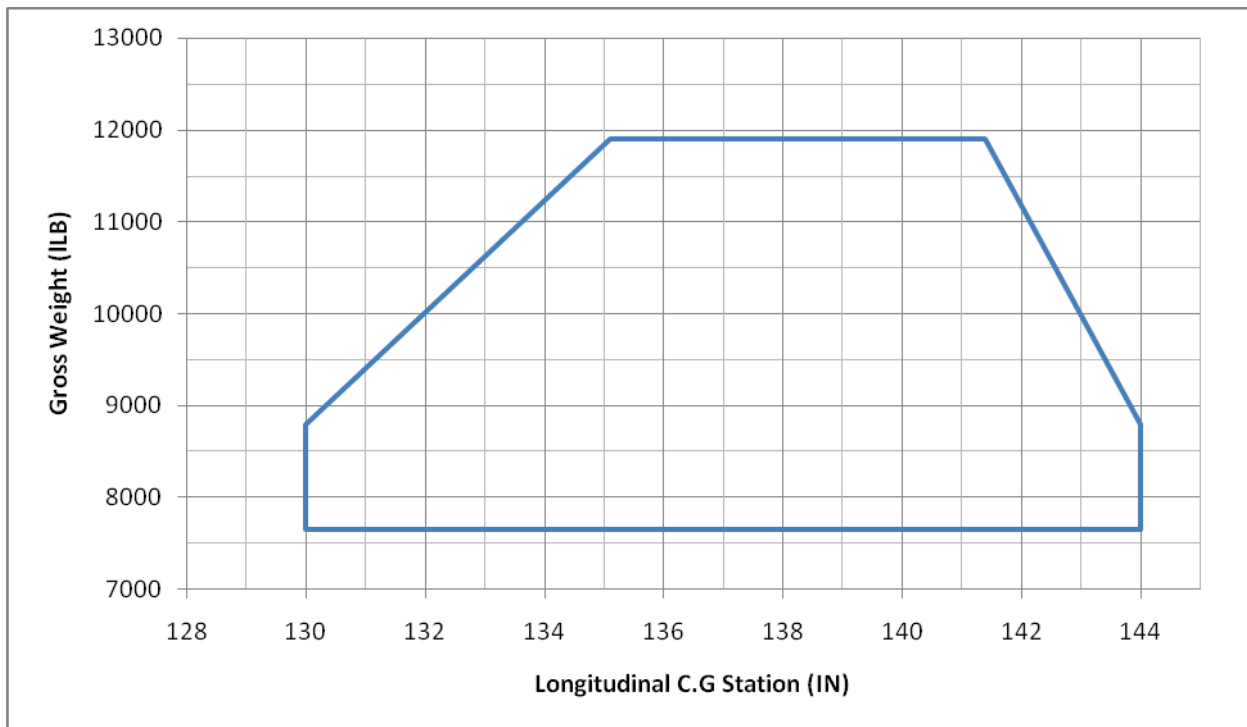


Figure 7.1. Gross Weight Center of Gravity Chart

7.2 Structural Design Criteria

As with other aspects of the Gyroblitz the structural design of this derivative aircraft uses much of the baseline aircraft's features. This is done for quick development and lower development and manufacturing costs. When possible the existing structure of the Bell 412 was kept. The fuselage was modified where necessary to accommodate for the addition of four canards and extensive modifications were made to the tail structure. Structural design was done in CATIA, and structural analysis was performed in ABAQUS.

7.3 Fuselage Design

The primary structure of the Bell 412 consists of two main longitudinal beams. These beams extend from the chin bubbles in the front to the mounting points for the tailboom, where they extend upwards to form the mounting structure for the transmission and mast assembly. The landing gear is mounted directly to the lower edge of these beams. Due to this design the structure of the Bell 412 was readily adapted to accommodate for the Gyroblitz changes. Loads are transferred to this primary structure through a conventional system of bulkheads, support beams and stringers and shown in Figure 7.3.

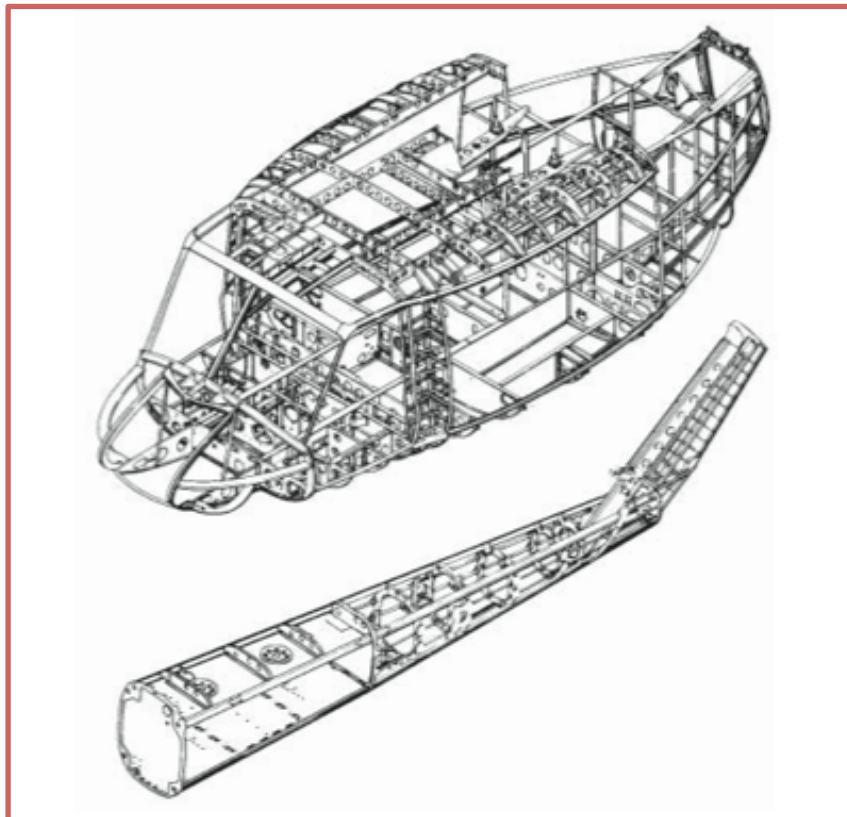


Figure 7.2. Structural skeleton of the Bell 412EP

The simple load paths of the Bell 412 allowed the tail and canard modifications to be made without a complex rearrangement of trusswork or a redesign of load paths. The canards are connected to the primary structure added using titanium pivot pins. The Primary beams additional doublers and mounting hardware at the canard mounting locations. This allows much of the same tooling that was used in production of the Bell 412 to be used in the manufacture of the Gyroblitz.

The aft structure of the Bell 412 is already the bulkiest structure on the aircraft, and most of the mast loads are transferred through the vertical portion of the main beams in the rear, rather than the bulkheads and box beams. The Gyroblitz thrust loads are generated through the tail at during forward flight rather than the mast, but the load paths in the fuselage are similar. From the tailboom mount the load is distributed to the rest of the aircraft through the main two longitudinal beams. No modifications to the existing fuselage structure were needed to accommodate for the increased loads generated by the tail in forward flight. Loading in hover is identical to that of the Bell 412, when the tail is being used in an anti-torque configuration.

The primary and secondary structure of the Gyroblitz is corrosion resistant aluminum alloy such as 7075-T6. Other materials are used in high stress areas, and high temperature areas. Titanium alloys are used on the workdeck, and for the canard pivot pins. Stainless steel is used on the engine deck for firewalls. Fiberglass is used in non-structural areas and as a face skin on honeycomb panels. The work deck is composed of a honeycomb sandwich with a titanium upper skin, and an aluminum honeycomb and fiberglass lower skin. Honeycomb construction is used in places where the skin panels bear structural loads, in these cases the outer skin is fiberglass and the inner skin is aluminum with additional aluminum doublers as needed.

7.4 Landing Gear Design

The landing gear is identical to that of the Bell 412. It is a skid landing gear made consisting of two longitudinal aluminum skid tubes, and two-arched aluminum cross tubes. The landing gear absorbs energy through elastic deflection of the cross tubes. The aft cross-tube is supported by a single beam on a single fitting which allows the gear to rock side to side mitigating ground resonance.

7.5 Validation/Analysis

7.5.1 Tail Structure analysis

The tail structure was the most heavily modified of all the structural components in this derivative aircraft. The tail structure needed to be increased to accommodate for the additional weight of the larger propeller at the rear, as well as the larger drivetrain system associated with its control. Additionally during forward flight the tail is generating all of the trust loads and needs to stay rigid to enable control of this inverted pendulum configuration.

In order to meet the requirements of these increased loads additional ribs were added to provide rigidity to an entirely honeycomb composite skin structure. Additionally two longitudinal rods were added to the two rods already in place in the Bell 412. The rigid honeycomb skin meets the torsional and bending load requirements, while the additional longitudinal beams meet the additional compression load seen during forward flight. Figure 7.4 shows a view of the skinless beam structure as well as the loads applied by the rotor in forward flight and hover conditions. Bonded honeycomb is chosen as a material rather than more advanced composite structures because it is already used elsewhere on the Bell 412, and by keeping the materials the same the Gyroblitz can be manufactured in the same shops and tested by the same equipment, essentially lowering maintenance cost.

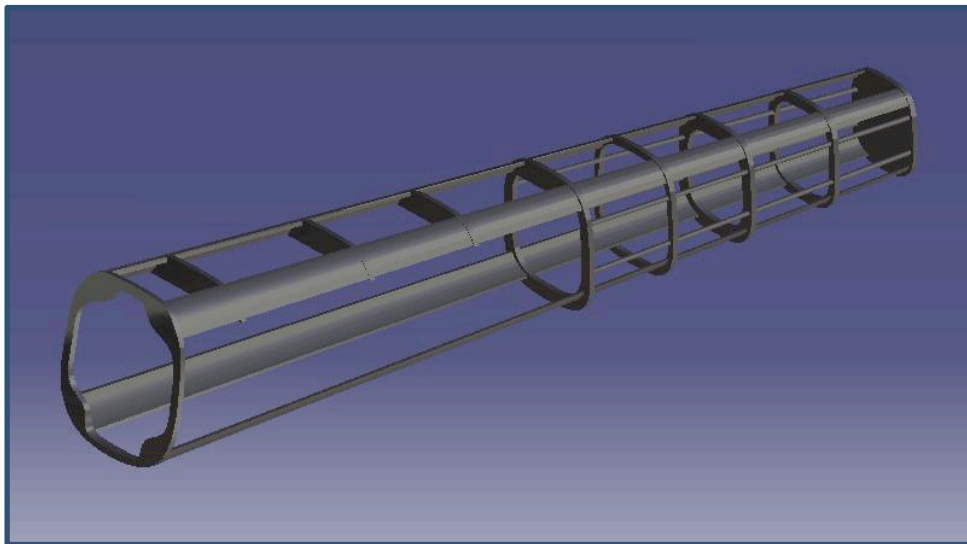


Figure 7.3. Gyroblitz tail structure.

8. Cost Analysis

Estimating the cost of a new design is vital to its success, whether it is a prototype of a new technology or a commercial or military product. This is reflected in the OEC mentioned in section 2. As shown in the OEC, cost is not a monolithic item, but rather is broken into three main sections described below:

- **Development Costs (Non-Recurring)**

- Initial Design, Prototype, Flight Test & Administrative Costs

- **Production Costs (Recurring)**

- Manufacturing Costs Including Subcontracting & Labor

- **Operating Costs (Recurring)**

- Flight Crew, Fuel & Oil, Maintenance & Repair, Depreciation

Each of these sections has been calculated using the Bell PC Cost Model and together form the *Life Cycle Cost* of the design. This set of numbers represents the total cost incurred throughout the aircraft's entire program.

8.1 Development Costs

The development cost of the design represents the amount of money sunk before the first unit is produced. This is detailed in Figure 8.1 below.

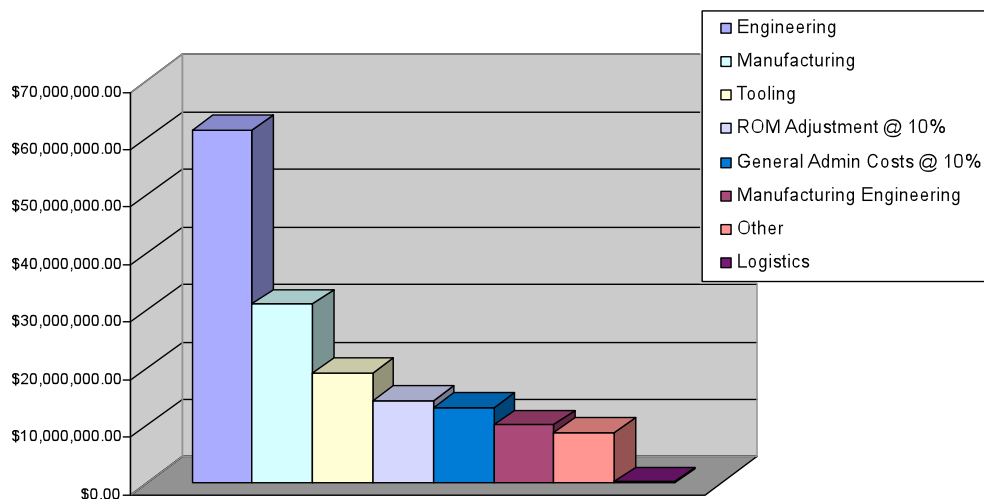


Figure 8.1. Development Cost Breakdown

The cost of engineering dominates the development costs, at more than twice the next expensive item, manufacturing. These numbers are in 2001 dollars, and have been totaled and adjusted for inflation in Table 8.1.

Table 8.1. Development Cost Summary

	Value
Development Subtotal	\$130,800,428
10% ROM Adjustment	\$13,080,000
10% General & Admin Costs	\$14,388,143
Grand Total After Inflation	\$189,922,286

The development subtotal is simply the sum of all elements in the cost breakdown. The Rough Order of Magnitude (ROM) and General & Administrative Costs are then added consecutively, allowing for a certain degree of uncertainty in the initial estimate. The final estimate is then corrected for inflation, coming to almost \$190 million dollars.

8.2 Production Costs

The recurring cost of manufacturing and assembling the helicopter are detailed in Figure 8.2 below.

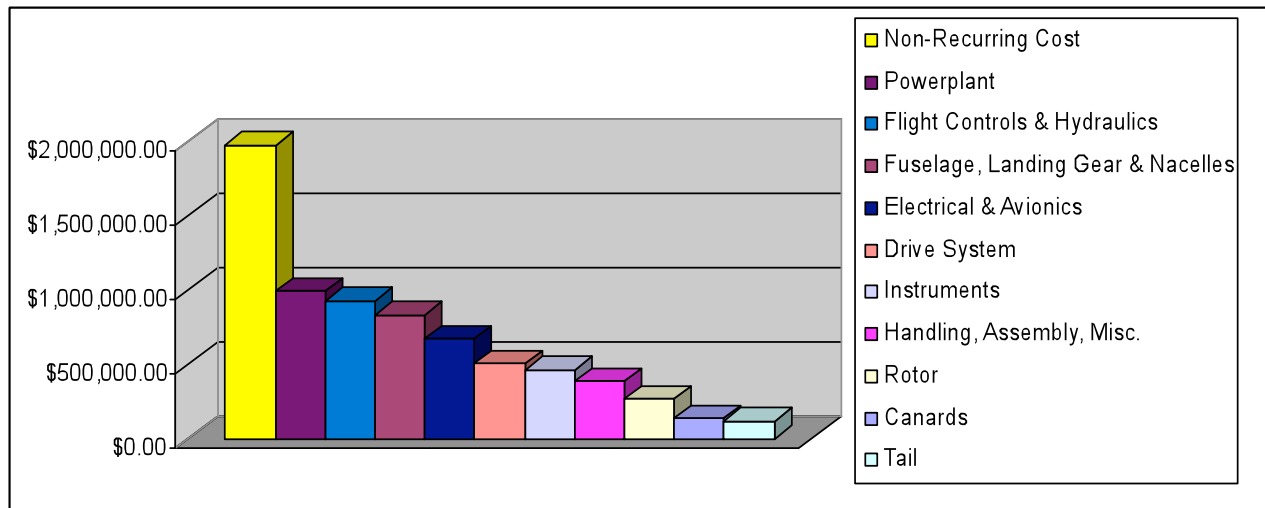


Figure 8.2. Production Cost Breakdown Averaged Over 80 Units

Of note is the significance of the non-recurring cost, shown in the figure for the sake of comparison. For an estimate of 80 units the development cost per unit far exceeds any other cost encountered in production. The breakdown of the other components of the helicopter is

more regular, with the power plant as the most expensive component, followed by the wide variety of flight controls, actuators & hydraulic systems found in the design. The Misc. section includes air induction, air conditioning and furnishings.

The averaged cost will go down if the non-recurring development cost is amortized over a larger production. To get a quantitative assessment of the difference in price, Figure 8.3 gives the average cost over a production of 350 units.

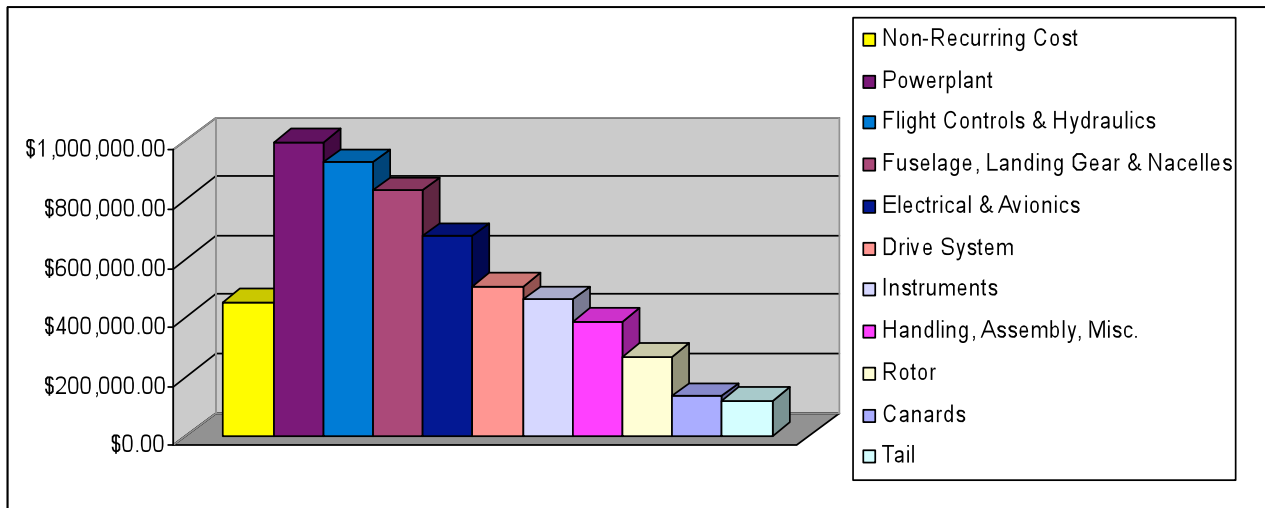


Figure 8.3. Production Cost Breakdown Averaged Over 350 Units

Table 8.2 will highlight what is shown in the figure above, that average unit cost is highly dependent on the number of units produced.

Table 8.2. Production & Unit Cost Comparison

	Value
Total Production Cost	\$6,363,916
Average Unit Cost: 350 Units Produced	\$6,906,552
Average Unit Cost: 80 Units Produced	\$8,737,945

This assumes that no further manufacturing cost reduction is attained after the production of 80 units, in that the cost to manufacture each unit does not change after the 80th unit. Figure 8.4 further explains the manufacturing composition the larger items (non-recurring cost aside) from Figure 8.3.

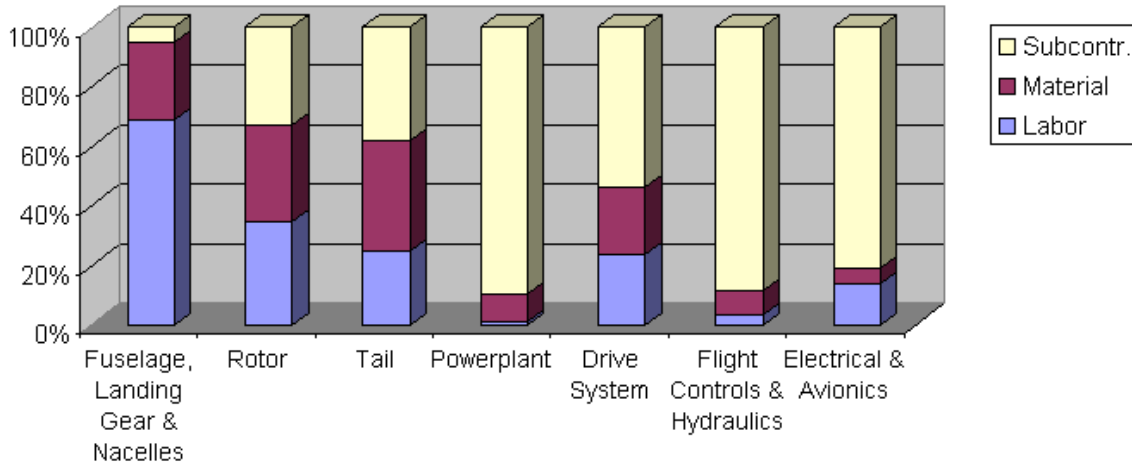


Figure 8.4. Production Cost Summary by Type

9. Safety and Certification

The Gyroblitz meets the Federal Aviation Regulations, specifically FAR part 27. Part 27 describes the airworthiness standards for a normal category rotorcraft. The weight requirements are selected by the group and make for a minimum weight of 7,651 lb and a maximum weight of 11,900 lb. The Gyroblitz is a derivative design based on the Bell 412, which has already been proven airworthy under FAR Part 27. Because of this, any parts of the aircraft that have not been changed can be assumed to be compliant.

The Gyroblitz is a derivative aircraft. Much of the aircraft has not changed, and since the root aircraft, the Bell 412 met FAR part 27, the subsequent requirements are also met by the Gyroblitz. The center of gravity has moved on far on the x-axis or z-axis. The only axis of concern is the Y-axis, and the larger tail structure on the aircraft. The large tail structure does not add enough weight to move the center of gravity as relocation of subsystems and a change of material to the tail shaft ensured stagnation for the center of gravity. The empty weight of the aircraft has increased 762 lb. When dry, the aircraft will weight 7,651 lb, and center of gravity remains the same as in the Bell 412. The max main rotor RPM and the pitch limits have not been changed from the Bell 412.

The Gyroblitz uses the same engines, the Pratt and Whitney PT-6 twin-engine system as the Bell 412. The take off and hover process has not been altered, and is therefore still compliant, in all engines operative and one engine inoperative states. Glider performance has been improved from the Bell 412 with the addition of the 4 canards.

The aircraft has been designed to meet or exceed the 1.5 safety factor required. The loads on aircraft in hover and low speed flight have not changed from the Bell 412. In high speed,

autogyro flight, the loads are lower on the rotor and in hover, and therefore meet the requirements. The structural strength has not been changed and no additional, extreme loads occur. The landing gear of the aircraft is a landing strut, and is capable of holding the additional weight, up to max gross weight of the Bell 412. The Gyroblitz has the same maximum gross weight as the Bell 412. The addition of the canards applied additional stress at the canard fastening locations. These locations have been proven to hold their required loads and the additional safety factor required by the FAR.

The engines already meet the FAR requirements and are used in the same context as before in the Bell 412.

The power plant has not been changed from the Bell 412. The additional gearing needed to power the tail rotor in forward flight meets safety requirements as described in section 5.

Equipment has not been changed from the Bell 412. All safety equipment is supplied and available for use, per the FAR requirements.

With the additional weight, canards and new autogyro system, the Gyroblitz still operates under the conditions of performance at minimum operating speed. The Gyroblitz maintains a steady rate of climb in all flight conditions. The landing requirements are met, as well as the speed envelope, autorotation requirements are met by not changing that part of the aircraft.

Construction of the Gyroblitz requires few special parts outside of the scope of the already in service Bell 412 construction facilities. The new, carbon fiber drive shaft to the tail rotor is made of an aircraft grade high strength carbon fiber-epoxy matrix, aligned with the predicted torsion angle inflicted on the drive shaft. The tensile strength and modulus exceed the safety factor of 1.5. It even exceeds the strength requirements if the engine torque is maxed out at 1.25 times max continuous torque. The modern carbon fiber composites are standard production grade.

The flight characteristics of the Gyroblitz are the same as the Bell 412 in low speed flight. Once the aircraft enters the autogyro regime, additional controls become available. The blade controls are the same, but a fly-by-wire system has been implemented to assist with the 4 moveable canards. The rotated tail rotor system does not add a significant amount of instability to the forward flight controls, and is automatically corrected by a simple "inverted pendulum" control. The rotor blades have not been changed from the Bell 412, and are therefore, compliant. The ground and water handling characteristics have not been changed.

10. Conclusion

The Gyroblitz is an appropriate name for a helicopter capable of auto-rotating in forward flight at a substantially fast cruise speed. The design of the Gyroblitz is a clear demonstration of innovation for the sake of performance. As outlined throughout the conceptual development of the Gyroblitz, innovation for the sake of innovation often meant a sacrifice in performance. The 2009 AHS competition called for innovation with the objective of increased performance and it is clear the Gyroblitz has satisfied both requirements.

The design process of the Gyroblitz involved researching a wide variety of technologies. This process yielded very valuable results, not necessarily because these results showed potential and were beneficial to performance, but because they exposed pointless technological concepts. In today's eco-friendly, earth-smart world, the idea of a hybrid helicopter or fully electric helicopter seems like a necessary quest. It should be noted that unfortunately, with today's technology, no matter how advanced it is, is still nowhere capable of handling the demands of rotorcraft. Today's batteries are leagues behind the amount of energy required to operate medium utility rotorcraft. The results of the Gyroblitz also show how unnecessary it is to develop a variable RPM or continuously variable RPM transmission for rotorcraft as the end results are only slightly more advantageous than the current transmission workings.

The Gyroblitz is successful in efficiently merging forward flight and hover capabilities into a single system. The potential for this single system is great and can only lead to further breakthroughs in rotor simplicity and combinations of separate systems.